PhD-FSTC-2017-30
The Faculty of Sciences, Technology and Communication

DISSERTATION

Defence held on 11/05/2017 in Luxembourg

to obtain the degree of

DOCTEUR DE L'UNIVERSITÉ DU LUXEMBOURG

EN SCIENCES DE l'INGENIEUR

by

Amalya Khurshudyan
Born on 29 May 1988 in Yerevan , Armenia

COMPARATIVE STUDY OF REDUCED ORDER METHODS FOR GEOMETRICALLY NON-LINEAR STRUCTURES

Dissertation defense committee

Dr Andreas Zilian, dissertation supervisor
Professor, Université du Luxembourg

Dr Salim Belouettar
Researcher, Luxembourg Institute of Science and Technology

Dr Stephane Bordas, Chairman
Professor, Université du Luxembourg

Dr Antoine Legay
Professor, Le Cnam

Dr Davide Baroli, Vice Chairman
Researcher, Université du Luxembourg

Abstract

The dissertation is devoted to the comparison and development of techniques for model order reduction (MOR) of geometrically nonlinear elastic structures in the static limit.

The MOR procedure works in the following way: the structure is first discretized into finite elements and a discretized system of algebraic equations is obtained, in which the stiffness matrix depends on the unknown vector. The system is then projected to a lower order space. The choice of the basis of the projection space is made according to the methods developed in the thesis. To this end, three techniques are developed here based on different choices of the basis functions.

Comparative analysis of the suggested methods is carried out in the case of two-dimensional structures (Euler-Bernoulli beam, multi-span beam and frame). In order to be able to compare the results with those obtained by the MOR techniques which are developed, the benchmark problems which are examined are first solved analytically.

Results of computations carried out in Python and are then discussed.

Contents

List of Figures

List of Tables

List of Symbols

The main notations used in the thesis are listed below:

$\mathbb{R}^n$	n dimensional Euclidean space
span $(\boldsymbol{V})$	intersection of all subspaces in a vector space containing the set of vectors $\boldsymbol{V}$
diag (a_i)	diagonal matrix with components $a_{ij} = a_j \delta_{ij}$
Superscript T	transposition
δ_{ij}	Kronecker's delta symbol
Id	identity matrix
$\boldsymbol{\sigma}$	Cauchy stress tensor
σ_{11}, σ_{22}, σ_{33}	normal Cauchy stresses
σ_{12}, σ_{13}, σ_{23} or τ_{12}, τ_{13}, τ_{23}	shear Cauchy stresses
$\boldsymbol{t}$	traction vector
$\boldsymbol{\varepsilon}$	Green-Lagrange strain tensor
ε_{11}, ε_{22}, ε_{33}	normal strains
ε_{12}, ε_{13}, ε_{23} or γ_{12}, γ_{13}, γ_{23}	shear strains
$\boldsymbol{\varphi}$	deformation vector
$\boldsymbol{u} = (u \;\; v \;\; w)^T$	displacement vector
$\boldsymbol{i}$, $\boldsymbol{j}$, $\boldsymbol{k}$	unit coordinate vectors of Cartesian system
$\boldsymbol{n} = (n_x \;\; n_y \;\; n_z)^T$	outer unit normal vector
$\boldsymbol{x} = (x \;\; y \;\; z)^T$	spatial Cartesian coordinate

$\mathbf{T}$	first Piola-Kirchhoff stress
$\mathbf{P}$	second Piola-Kirchhoff stress
W	strain energy density
E	Young‘s or elastic modulus
λ, μ	Lamé coefficients
I	cross sectional moment of inertia
A	area of cross section
h	thickness
ν	Poisson‘s ratio
Q or N	sectional force
M	bending moment

Chapter 1

Introduction

There are various important reasons why predictive modelling and analysis of engineering structures is necessary before they are constructed and put to use: stable performance of the structure, lifetime estimation, wear prognosis and so on.

Choice of the model for a structure under consideration depends on what type of loading it will be subjected to (compression, stretching, bending, torsion, etc.) and how it is linked to neighbouring elements. In general, mathematical models of static structures under loading are boundary value problems. Ideally, for complete structural analysis, the model equations are solved analytically, which is sometimes too complicated. This difficulty provides the motivation to develop efficient and accurate numerical methods for computational approximation of such problems. Currently, there exist various numerical methods for approximating boundary value problems for differential equations, providing different accuracies and requiring different computational costs. Depending on the problem under consideration, in order to reduce complexity, an approximate solution with relatively less accuracy might be sufficient. In structural analysis, however, where the accuracy of the calculations is very important, other ways of reducing complexity have been developed.

One of the most efficient and preferred techniques for reducing the computational costs without significantly affecting accuracy is model order reduction (MOR), which

involves approximating the original model by reducing the dimension of its discrete state space (or degrees of freedom). As a result, the reduced order model can often be evaluated in significantly less time, but with lower accuracy compared to the original high-fidelity model.

1.1 Motivation

Closed-form solutions for boundary value problems arising in Structural Mechanics are difficult and sometimes impossible to obtain. This is not only because of non-linear terms present in the equilibrium equations, but also because of the geometrical complexity of the problem domain. To obtain approximate solutions, discretization methods are generally used and the governing system is transformed into a system of algebraic equations. With such approaches, the accuracy of the approximation depends on the discretization: the finer the discretization, the more accurate the approximation and the higher the dimension of the discrete system.

Depending on the complexity of the problem or the required accuracy of the approximation, many degrees of freedom may be necessary. Eventually, the number of unknowns may range between hundreds to several millions. Therefore, the solution will require huge computational effort. The most significant motivation for model order reduction methods is to reduce the computational costs associated with the solution for obtaining higher dimensional systems.

1.2 State of the Art

Depending on complexity of the problem, numerical simulations might be very time-consuming. Therefore, applied scientists and engineers clearly need to develop approaches which somehow enable them to reduce the complexity of computations, while preserving the desired characteristics of the model (e.g. stability, continuous dependence on crucial parameters, etc.), and avoiding altering the accuracy. MOR methods play an indispensable role in such cases.

The general idea of MOR is to approximate a discrete system of higher dimension n by a reduced system of lower dimension k, so that $k \ll n$, which ideally has the same behaviour as the original (see, for instance, [6]). The original system can be linear or non-linear, stationary or non-stationary [56].

A typical model reduction process involves creating a suitable reduced basis depending on the objective of the problem and the actual reduction algorithm itself. There are some requirements which have to be met while constructing the basis and performing the reduction algorithm, such as preserving the main characteristics of the system, the approximation error associated with the reduced model should be small, and the reduction techniques should not be computationally expensive to perform, etc. [28].

For linear systems the reduction is usually a one-step procedure, since the matrices and vectors describing the behaviour of the system do not depend on the vector of unknowns [34]. Conversely, in the case of non-linear systems, the coefficient matrix definitely depends on the vector of unknowns. MOR then becomes part of an iterative procedure, and at each step of this procedure the coefficient matrix will be different but constant [43]. Therefore, by applying a particular MOR method for a linear system at each step of the iteration, a non-linear system can be approximated. Thus, the whole iteration procedure can be viewed as a sequence of linear problems [42]. The latter approach will remain computationally expensive because

of the need to generate a basis at each step.

The main classes of model order reduction techniques for linear systems are based on the Krylov subspace method [63], Hankel norm approximants [29, 30] and Karhunen-Loeve expansion, which is also called proper orthogonal decomposition (POD) [53].

The methods dealing with non-linear systems include the empirical methods [51], linearisation methods [19], trajectory approximation methods [25] and parametrization approach [27].

1.2.1 Model-Order Reduction for Linear Systems

In this subsection, several MOR methods used for approximation of linear non-stationary systems are summarized. The main definitions and formula representations of all the main terms used in this subsection are presented and fully explained in [6, 37, 56].

1.2.1.1 MOR Algorithms Based on Krylov Subspace Method

The first MOR method based on Krylov subspace is so-called Asymptotic Waveform Evaluation (AWE). This method involves Padé approximation to approximate the transfer function of the system. This method consists of two steps. First, the moments of the transfer function expansion are computed in terms of its poles and then the coefficients of the approximating polynomials are determined via moment matching.

However, AWE has some disadvantages. In particular, its unstable numerical behaviour due to round-off errors, moment computations are explicit [61].

To overcome these difficulties, a modification of AWE is proposed in [59], using in Padé approximation the two-sided Lanczos procedure [10] instead of moment matching, which is too costly. This method, called the Padé-via-Lanczos (PVL)

method, is more robust and generates more poles, although it still requires the same computational effort as AWE [44]. It overcomes the loss of accuracy as k increases, it avoids the singularities in Padé tables and improves the quality of approximation of the frequency response away from the Padé expansion frequency [58]. Nevertheless, since PVL is based on two-sided Lanczos algorithm and non-orthogonal projections, it does not always preserve the stability of the system. To overcome this disadvantage To overcome this disadvantage, it is suggested that Ruth tables are used instead of Padé's. This method involves no eigenvalue analysis (see [45] and the references therein).

All these methods involve rewriting the higher-order system in the form of an equivalent larger first-order system and applying reduction algorithms. Even although a good approximation can be obtained, it does not preserve the form of the higher-order systems. A new approach based on Krylov subspace projection techniques that preserves the form of the original higher-order system is presented in [61].

Consider a non-stationary linear discretized system of the form

$$\mathbf{B}\dot{\boldsymbol{x}}(t) + \mathbf{A}\boldsymbol{x}(t) = \boldsymbol{b}(t),$$

where $\boldsymbol{x}, \boldsymbol{b} \in \mathbb{R}^n$, $\mathbf{A} \in \mathbb{R}^{n\times n}$, t represents the time. The matrix

$$\mathbf{Kr}\left(\mathbf{A}; \boldsymbol{v}\right) := \operatorname{span}\left(\boldsymbol{v}, \mathbf{A}\boldsymbol{v}, \ldots, \mathbf{A}^{k-1}\boldsymbol{v}\right) \in \mathbb{R}^{n\times k},$$

generated by some starting vector $\boldsymbol{v} \in \mathbb{R}^n$ is called the Krylov matrix. The Krylov subspace is spanned by the columns of $\mathbf{Kr}$. Later, in this thesis the column vectors of this matrix are orthonormalized and used as a projection basis.

For stability purposes, the matrix $\mathbf{A}$ must be symmetric. In the case of non-symmetric matrices $\mathbf{A}$, it is suggested in [23] that the Lanczos algorithm be used on the so-called left Krylov subspace, which, unlike $\mathbf{Kr}$, is spanned on $\mathbf{A}^T$ instead of $\mathbf{A}$. As is shown in [25], with the same aim it is also possible to shift and invert the Lanczos algorithm and apply it efficiently.

Another approach that works well for non-symmetric matrices is Arnoldi's method. In this case the basis is generated in such a way, that the vectors remain orthogonal, even though this method does not always preserve the passivity of the system [21]. Some other approaches dealing with non-symmetric matrices are reviewed in [32].

All the advantages of Arnoldi's method were used to develop the Passive Reduced-Order Interconnect Macromodeling Algorithm (PRIMA) method. To generate an orthonormal basis, PRIMA uses Arnoldi's method; the corresponding Krylov space is therefore the same as in the Arnoldi method and PVL. However, unlike these methods, the projection of the matrices is explicit in PRIMA. This is a minor disadvantage in the sense that explicit projections are more expensive. Nevertheless, it makes PRIMA more accurate compared with Arnoldi's method and, moreover, it preserves the stability and passivity of the system. On the other hand, even though unlike PVL it preserves only one moment at each iteration, it operates with $\mathbf{A}$ only, while PVL has to operate also with $\mathbf{A}^T$.

A modification of PRIMA, Structure Preserving Reduced order Interconnect Macromodeling (SPRIM) is suggested in [62]. The paper reviews both methods and shows the advantages of the latter.

Several other algorithms using the Krylov subspace method for solving initial value problems and providing a priori error estimates can be found in [15] and [63], as well as references therein. These methods are applied efficiently in the simulation of linear [60] and non-linear [36] circuits, turbulent flows [24], structural dynamics [23], and the numerical integration of large systems of differential equations [20], etc.

More details on Krylov subspace techniques and practical projection algorithms can be found in Chapter 4 of this thesis.

1.2.1.2 Methods Based on Hankel Norm Approximants and Truncated Balancing Realization (TBR)

The controllability and observability Gramians associated with the linear time-invariant system $(\mathbf{A}, \mathbf{B}, \mathbf{C}, \mathbf{D})$ are defined as follows:

$$\mathbf{P} = \int_0^\infty \exp\left[\mathbf{A}t\right] \mathbf{B}\mathbf{B}^T \exp\left[\mathbf{A}^T t\right] dt,$$

$$\mathbf{Q} = \int_0^\infty \exp\left[\mathbf{A}t\right] \mathbf{C}^T\mathbf{C} \exp\left[\mathbf{A}^T t\right] dt,$$

which are the unique solutions of the following Lyapunov equations [56]:

$$\mathbf{A}\mathbf{P} + \mathbf{P}\mathbf{A}^T + \mathbf{B}\mathbf{B}^T = \mathbf{0},$$

$$\mathbf{A}^T\mathbf{Q} + \mathbf{Q}\mathbf{A} + \mathbf{C}^T\mathbf{C} = \mathbf{0},$$

arising from stability assumptions on $\mathbf{A}$. Stability in the matrix $\mathbf{A}$ implies that the defined improper integrals are bounded.

After determining the matrices $\mathbf{P}$ and $\mathbf{Q}$, a state space transformation balancing the system, i.e. providing $\mathbf{P} = \mathbf{Q} = \mathrm{diag}\,(\sigma_i)$, where σ_i are the so-called Hankel singular values, must be determined. If starting from some i, $\sigma_i < \sigma_{i+1}$, then the axis corresponding to σ_{i+1} is more easily controllable and observable. Therefore, by neglecting values starting from $k+1$, a k-dimensional reduced order model can be derived. However, one of the disadvantages of this method is, that the solution of the Lyapunov equations is computationally expensive [50], although it does give the best approximation when the whole frequency range is considered [5]. See also the survey [54].

1.2.1.3 Optimal Hankel Norm Reduction

The truncated system obtained using the TBR method is not necessarily an optimal approximation. Optimal Hankel norm reduction method proposes an optimality

criterion in the form of the so-called Hankel norm. For the Hankel operator [56]

$$\boldsymbol{y} := \mathcal{H}\left[\boldsymbol{u}\right] = \int_{-\infty}^{0} \mathbf{H}(t-\tau)\boldsymbol{u}\left(\tau\right) d\tau,$$

where $\mathbf{H}(t) := \mathbf{C}\exp\left[\mathbf{A}t\right]$ when $t \geq 0$, the Hankel norm is defined by

$$\left|\left|\boldsymbol{\Sigma}\right|\right|_H = \sup_{\boldsymbol{u}\in L^2(-\infty,0)} \frac{\left|\left|\boldsymbol{y}\right|\right|_2}{\left|\left|\boldsymbol{u}\right|\right|_2}.$$

Since the characteristics of these methods are functions of time, it is used for dynamical systems only.

1.2.1.4 Techniques Using Karhunen-Loeve Expansion (POD)

Karhunen-Loeve expansion, also known as Proper Orthogonal Decomposition (POD) is based on Singular Value Decomposition (SVD), which involves approximating matrices by matrices of lower rank. The first step when using this method is to construct a matrix containing column vectors describing the state of the system at certain given instants, often referred to as snapshots. The snapshots are solutions to the large problem and are considered to be close to the nature of the problem to be reduced. They are mostly already available (e.g. extracted from experiments), which reduces the POD methods mostly posterior . Once the snapshot matrix has been constructed, its singular value decomposition provides the vectors corresponding to the largest singular values. These vectors can be used as the basis for POD method.

Studies show that POD can be successfully combined with other model order reduction techniques, for example, with balanced reduction method to minimize computation costs by approximating the Gramians by snapshot method instead of computing the exact ones [26, 57]. This approach is computationally more efficient, but applicable only if a small number of outputs are considered. The effect of perturbations in the snapshots is discussed and the sensitivity of the system to these perturbations is studied in [26]. It was shown that the method is not efficient

if the database is being updated, similar to POD applied to nonlinear problems [47]. To avoid this disadvantage, an algorithm is suggested in [4] which constructs the basis functions incrementally.

The POD method is therefore a very convenient method for linear systems, but for non-linear systems the snapshots should be recalculated to update the stiffness matrix. It can be overcome by the so-called proper generalized decomposition (PGD) method introduced in [41]. This is an a priori approximation, which does not rely on knowledge of the solution for the whole problem. It makes it possible to enrich the reduced approximation basis in order to improve the accuracy. To avoid using this stiffness matrix updating procedure, a combined POD-ANM (Asymptotic Numerical Methods) procedure is proposed [40].

The so-called goal oriented optimization approach, developed in [55], has several advantages over the POD method. One of these advantages is that it targets the projection basis to output functionals of interest by treating the reduced order governing equations as constraints for determination of the basis and it provides a framework to deal with multiple parameter instances.

1.2.2 Model Order Reduction of Non-linear Systems

Some of the methods developed for linear problems can be adapted and used for non-linear problems. In this subsection, some MOR methods for non-linear systems are discussed.

1.2.2.1 Empirical Methods

A method based on empirical Gramians is introduced in [16]. It uses empirical Gramians, which define the non-linear behaviour of the system near an operating point. Then, the less important states are reduced using a Galerkin projection. One of the advantages of this technique is that it can be applied to non-linear systems,

while requiring only linear matrix computations. As shown in [51, 52], the TBR can be combined with Karhunen-Loeve techniques for reduction of nonlinear systems. It should be noted that if the system is linear, this method coincides with the ordinary TBR.

Gappy POD is another combined non-linear reduction method. It was originally developed for face recognition and evaluates only a small subset of nonlinear functions. The other entries are reconstructed by an interpolator or a least squares strategy using a pre-computed reduced-order basis [7].

Another MOR method for non-linear systems is the Gauss–Newton with approximated tensors (GNAT). The dimension reduction is achieved using the Petrov-Galerkin projection and gappy POD technique [11]. The right reducing basis is constructed by POD. The left one is chosen to minimize the residual of the linearized system at each step of the Newton iteration. To decrease the computational cost, the non-linear residual and jacobian on the right reduction basis are approximated by gappy POD. In [7] the method is applied to a non-linear structural dynamical system. It is further developed in [11] for turbulent viscous flows. The finite volume method is chosen to discretize the system.

Another empirical MOR method applied directly on the non-linear term is the Discrete Empirical Interpolation Method (DEIM) developed in [49]. It is another POD combined method. The DEIM is interpolating the reduction subspace obtained by POD, which approximates the space of nonlinearities (see also [53]). This is often referred to as direct approach. An unassembled variation of this method is applied directly to the non-linear term before the discrete operator is assembled. Both approaches have their advantages and disadvantages. In particular, the possibility of selecting the collocation points automatically from the full set of DOF is an advantage. If many elements share the same DOF, then an unassembled approach is chosen, because the direct approach leads to selection of a high number of finite elements. Therefore, the subspace of unassembled non-linear internal forces is of a

higher dimension. On the other hand, some of the reduced responses are unstable for unknown reasons.

1.2.2.2 Linearization Methods

As mentioned above, non-linear terms can be expanded into a sequence of linear ones and a MOR method for linear system can be applied to each term in the sequence. Common methods of linearization techniques are the Volterra method [46], incremental linearization method, trajectory approximation method [25], Newton-Raphson linearization [39] (see also paragraph 3.2.2.2 for details), etc.

1.2.2.3 Reduced Basis Methods

RReduced basis decouples the generation and projection stages of reduced basis approximation and eventually leads to computational savings. Using the reduced basis technique, the discretized structure response is defined through a non-linear system of finite element equations and a Rayleigh-Ritz technique is used to replace these equations by a reduced system with significantly fewer unknowns [31, 32, 62].

This is accomplished by approximating the n-dimensional solution vector by a linear combination of m linearly independent vectors. This set of global vectors is used as the basis in the order reducing projection algorithm.

An ideal set of basis vectors is defined as one which maximizes the quality of the results and minimizes the total effort spent on obtaining them. These basis vectors must be

- linearly independent,
- involve low computational costs in their generation,
- allow automatic selection of their number,
- provide a good characterization of the nonlinear response.

The basis vectors will be functions of derivatives of a path parameter. As the number of path derivatives increases, the basis vectors tend to become less linearly independent and their contribution to the solution accuracy diminishes.

The reduced basis computational procedure consists of *i)* determination of basis vectors and generation of the reduced system [3]; *ii)* characterization of non-linear response; *iii)* automatic selection of load step size and evaluation of corresponding nodal displacements and forces; *iv)* sensing and controlling the error in the reduced system; *v)* tracing post buckling and post-limit-point paths.

1.3 Purpose of the Study

In many structural engineering problems, having knowledge of selected eigenvalues corresponding to the governing system will suffice for basic dynamic analysis. In most cases, the smallest eigenvalues are of primary interest, as the smallest eigenvalue corresponds to the lowest oscillation frequency. The corresponding eigenvector defines the shape of the structure in the lowest mode. Often, the contribution of proceeding modes can be ignored method. Therefore, the solution of such problems may be described by an approximation of lowest eigenvalues and corresponding eigenvectors [33].

From this fact a number of developments arise as a consequence , such as power iteration (and other related) numerical methods. It is, in particular, used in vibration reduction for dynamical systems.

The main requirement of model order reduction for dynamic problems is to preserve dynamic stability properties [1]. The stability of dynamical systems is determined by the poles of the transfer function. Therefore, the main objective of MOR for dynamical systems is to approximate the transfer function of the original problem. Meanwhile, dynamic stability does not play any role for static systems, since the stability is completely different in terms of statics and dynamics. Stability in terms of statics is associated with the characteristics of the equilibrium path of the system, whereas in terms of dynamics it means that the system's output signal remains limited. Any static loading applied to structural systems will not change the dynamic stability in the system during a particular period of time. Therefore, it makes no sense to approximate the largest eigenvalues of the matrix representing a static system. Anyone wishing to adapt the MOR available for dynamical systems to static systems should follow this logic: the construction of the Krylov space is nothing other than power iteration method, which approximates the dominant eigenvalues of the discretization matrix; the corresponding eigenvectors, the so-

called Ritz vectors, can be a very good choice for a basis for dynamical systems. So, it is possible that using the inverse power iteration method while constructing the Krylov subspace can provide a good approximation.

Indeed, Antoulas in [6] suggests constructing an "inverse" Krylov subspace using $(\mathbf{A} - s\mathrm{I})^{-1}$ instead of $\mathbf{A}$ in its definition, where s is some guess of an eigenvalue for the matrix $\mathbf{A}$. Using the "inverse" subspace the lowest eigenvalues of matrix $\mathbf{A}$ is approximated and the eigenvectors corresponding to those eigenvalues are indeed a good choice of basis for static problems. But first of all, the computation of $\mathbf{A}^{-1}$ is very costly, and secondly- once we have the inverse of the discretization matrix, we will have the solution for the problem.

Therefore, the question can be put – is there any possibility of using MOR methods (at least some of them) for static problems? Can MOR offer an advantage for such problems? Computationally this might not be the case for static non-parametrized problems. However, the evaluation might be different for large parametrized and non-linear static problems. Is there a proper choice of a basis which makes it possible to cut computational costs while giving a good approximation for the static problem?

As has already been mentioned, statics and dynamics have different aims. However, there are also similarities. In the context of ROM of (non-linear) equilibrium paths of static structures, approaches previously developed for reduced order modelling of dynamic problems could be helpful if time is seen as the parameter evolving the system response along the equilibrium path. Such a parameter, for instance, can be the magnitude of an external force, its localization, the characteristics of the material, geometry, etc. By solving the parametrized problem for different values of the parameter, we eventually obtain a set of vectors representing the state of the system for different values of the parameter. A similar set is obtained for dynamical systems, containing the state of the system at different moments in time. It is the set of so-called snapshots, which is used in POD-based MOR methods.

For dynamical systems, snapshots are usually the result of experiments or other observations, and therefore are often given in advance. For static systems, they should be calculated first, it might not make any sense to solve the problem for different values of parameters in order to create a basis for MOR for static systems. Nevertheless, when the process is repeated many times it does become useful. For instance, many experiments are performed repeatedly during design verification and the required data can be obtained by means of sensors without any significant difficulties. In such cases, MOR becomes meaningful for static analysis. For example, it can be extremely helpful for static analysis of large systems such as plane wings or fuselage, because depending on the size of the construction it can take up to several days to do the calculations for it during non-linear static analysis.

Recent developments of MOR techniques show that POD can be applied to parametrized static systems. An improved POD method – so-called goal oriented compact POD – was suggested in [9]. This method uses sensitivity derivatives instead of state snapshots, and computation for this is less costly. In the paper some examples of optimization application are considered.

Parametrized MOR is studied for static analysis and control in [27]. As an example of static analysis a large reflector model and its shape control is considered to optimize the input control. Reduction uses the Krylov subspace technique. The projection basis is constructed using the initial loading as a starting vector. The accuracy of such approximation greatly depends on choice of starting vector.

An adaptive POD-Krylov reduced-order model is suggested in [8] for structural optimization problems. Approximate solutions of the state and sensitivity equations of the structure are evaluated at each step of the optimization loop via a POD-augmented conjugate gradient method. First, the solution component is computed in the POD subspace. By means of well conditioned reduced equations, fast convergence is ensured. In the final stage, the solution is refined in an adaptively computed Krylov subspace using an augmented preconditioned conjugate gradient

method. In order to achieve the prescribed accuracy level, the dimension of the Krylov subspace is increased.

This research is dedicated to a comparative study of reduced order methods for statics of geometrically non-linear structures. The aim is to identify reliable MOR algorithms, allowing for reduced order accurate approximation in static analysis of parametric problems. To be applicable to more general structures such as multi-span beams and frame structures, the algorithms must also be flexible.

1.4 Outline of the Thesis

Chapter 2 of the thesis is an introduction to the statics of structures. A general theory is considered and Euler-Bernoulli beam theory is derived for later consideration. Governing equations for linear and non-linear theories are presented.

Weak formulation for the governing equations of the Euler Bernoulli beam theory is derived in Chapter 3. To approximate the solution, the finite element method (FEM) is chosen. All the aspects of this method which serve the purpose of the thesis are described.

Chapter 4 considers a parametrized static system by introducing the so-called *offline* and *online* phases. Different techniques of projection method are discussed. Three reliable and flexible MOR methods for Statics valid for different types of beam structures are developed.

Some exemplary problems are considered, and rigorous solutions for these are obtained in order to verify the results obtained by approximation methods. These results are included in Chapter 5. Comparison between FEM approximation and MOR approximation, error estimation, as well as error sensitivity analysis is carried out for each method developed.

Finally, all the main findings of this work are summarized and conclusions are provided in the Summary and Conclusion.

Chapter 2

Statics of Structures

Statics of structures is a branch of structural mechanics which analyzes equilibrium states of a structure subjected to external loading. Static structural analysis is applicable in cases when a structure is subjected to a dead load, i.e. a load which is relatively constant in its magnitude and direction over an extended period of time. Alternatively, if the action of the loading varies in time and happens with negligible slowness, methods of static structural analysis [17] can still be used.

If a structure subjected to external loading is in static equilibrium, the sum of external and internal forces must be equal to zero. This equality provides constraints on unknowns, such as internal forces, moments, reactions, etc. Those constraints are called static equilibrium equations. For convenience, static equilibrium equations are usually written in differential form with respect to stress tensor components and are therefore often referred to as differential equations of static equilibrium.

Considering also material laws and kinematic relations in the framework of a particular structural theory, the full system of differential equations of equilibrium are obtained with respect to characteristic quantities of the stress-strain state of the structure as a coupled system of PDEs or ODEs (depending on the dimension of the structure). Uniqueness of solution for the full system of differential equations of equilibrium will require appropriate boundary conditions in addition.

2.1 Governing Equations of Solid Mechanics

In this section we derive differential relations obtained from equilibrium conditions with respect to stress tensor components acting in a point of elastic structure.

2.1.1 Kinematic Relations

Since the main assumptions of structural theories for beams, plates and shells are usually expressed in terms of the displacement field, for the derivation of governing differential equations, the relation between stress/strain tensor components and displacements is needed. The relations between strains and displacements are often referred to as kinematic relations

Kinematic relations describing large deformations of a structure are formulated by the Lagrangian finite strain tensor, also called the Green-Lagrange strain tensor. It is usually defined in terms of deformation gradient $\mathbf{F} = \nabla\boldsymbol{\varphi}$ [18]

$$\boldsymbol{\varepsilon} = \frac{1}{2}\left(\mathbf{F}^T\mathbf{F} - \mathrm{Id}\right),$$

or, equivalently, in terms of displacements [18],

$$\boldsymbol{\varepsilon} = \frac{1}{2}\left[\nabla\boldsymbol{u} + (\nabla\boldsymbol{u})^T + \nabla\boldsymbol{u}\cdot(\nabla\boldsymbol{u})^T\right]. \tag{2.1}$$

In Cartesian coordinate system (2.1) can be written component-wise as follows

$$\varepsilon_{ij} = \frac{1}{2}\left[\frac{\partial u_i}{\partial x_j} + \frac{\partial u_j}{\partial x_i} + \frac{\partial u_k}{\partial x_i}\frac{\partial u_k}{\partial x_j}\right] \tag{2.2}$$

(summation concept over k is accepted). In expanded form we obtain

$$\varepsilon_{11} = \frac{\partial u_1}{\partial x_1} + \frac{1}{2}\left[\left(\frac{\partial u_1}{\partial x_1}\right)^2 + \left(\frac{\partial u_2}{\partial x_1}\right)^2 + \left(\frac{\partial u_3}{\partial x_1}\right)^2\right],$$

$$\varepsilon_{22} = \frac{\partial u_2}{\partial x_2} + \frac{1}{2}\left[\left(\frac{\partial u_1}{\partial x_2}\right)^2 + \left(\frac{\partial u_2}{\partial x_2}\right)^2 + \left(\frac{\partial u_3}{\partial x_2}\right)^2\right],$$

$$\varepsilon_{33} = \frac{\partial u_3}{\partial x_3} + \frac{1}{2}\left[\left(\frac{\partial u_1}{\partial x_3}\right)^2 + \left(\frac{\partial u_2}{\partial x_3}\right)^2 + \left(\frac{\partial u_3}{\partial x_3}\right)^2\right],$$

$$\varepsilon_{12} = \frac{1}{2}\left[\frac{\partial u_1}{\partial x_2} + \frac{\partial u_2}{\partial x_1} + \frac{\partial u_1}{\partial x_1}\frac{\partial u_1}{\partial x_2} + \frac{\partial u_2}{\partial x_1}\frac{\partial u_2}{\partial x_2} + \frac{\partial u_3}{\partial x_1}\frac{\partial u_3}{\partial x_2}\right],$$

$$\varepsilon_{13} = \frac{1}{2}\left[\frac{\partial u_1}{\partial x_3} + \frac{\partial u_3}{\partial x_1} + \frac{\partial u_1}{\partial x_1}\frac{\partial u_1}{\partial x_3} + \frac{\partial u_2}{\partial x_1}\frac{\partial u_2}{\partial x_3} + \frac{\partial u_3}{\partial x_1}\frac{\partial u_3}{\partial x_3}\right],$$

$$\varepsilon_{23} = \frac{1}{2}\left[\frac{\partial u_2}{\partial x_3} + \frac{\partial u_3}{\partial x_2} + \frac{\partial u_1}{\partial x_2}\frac{\partial u_1}{\partial x_3} + \frac{\partial u_2}{\partial x_2}\frac{\partial u_2}{\partial x_3} + \frac{\partial u_3}{\partial x_2}\frac{\partial u_3}{\partial x_3}\right].$$

Obviously, $\boldsymbol{\varepsilon}$ is symmetric, i.e. $\varepsilon_{ij} = \varepsilon_{ji}$.

In geometrically linear structural theories, the last term on the right hand side of (2.2) is neglected due to:

$$\frac{\partial u_k}{\partial x_i}\frac{\partial u_k}{\partial x_j} \ll 1,$$

and the following *linear* kinematic relations follow

$$\begin{gathered}\varepsilon_{11}^{lin} = \frac{\partial u_1}{\partial x_1},\ \varepsilon_{22}^{lin} = \frac{\partial u_2}{\partial x_2},\ \varepsilon_{33}^{lin} = \frac{\partial u_3}{\partial x_3},\\ \varepsilon_{12}^{lin} = \frac{1}{2}\left[\frac{\partial u_1}{\partial x_2} + \frac{\partial u_2}{\partial x_1}\right],\ \varepsilon_{13}^{lin} = \frac{1}{2}\left[\frac{\partial u_1}{\partial x_3} + \frac{\partial u_3}{\partial x_1}\right],\ \varepsilon_{23}^{lin} = \frac{1}{2}\left[\frac{\partial u_2}{\partial x_3} + \frac{\partial u_3}{\partial x_2}\right].\end{gathered} \tag{2.3}$$

2.1.2 Balance of Linear Momentum

Let a body force $\boldsymbol{F} = (F_1, F_2, F_3)$ be acting on the differential volume element $d\boldsymbol{x} = dx_1 dx_2 dx_3$ of a continuous body Ω, which is described in the Cartesian coordinate system in reference (or undeformed) configuration. Then equilibrium of forces in that element provides [17, 18]

$$\frac{\partial \boldsymbol{t}_1}{\partial x} d\boldsymbol{x} + \frac{\partial \boldsymbol{t}_2}{\partial y} d\boldsymbol{x} + \frac{\partial \boldsymbol{t}_3}{\partial z} d\boldsymbol{x} + \boldsymbol{F} d\boldsymbol{x} = \boldsymbol{0}.$$

Here

$$\boldsymbol{t}_1 = \sigma_{11}\boldsymbol{i} + \sigma_{12}\boldsymbol{j} + \sigma_{13}\boldsymbol{k},$$

$$\boldsymbol{t}_2 = \sigma_{21}\boldsymbol{i} + \sigma_{22}\boldsymbol{j} + \sigma_{23}\boldsymbol{k},$$

$$\boldsymbol{t}_3 = \sigma_{31}\boldsymbol{i} + \sigma_{32}\boldsymbol{j} + \sigma_{33}\boldsymbol{k},$$

are the traction vectors, expressed in terms of the components of the first Piola-Kirchhoff stress tensor $\boldsymbol{\sigma}$.

Since the equality holds for arbitrary differential volume element $d\boldsymbol{x}$ of the continuum, and the unit vectors $\boldsymbol{i}$, $\boldsymbol{j}$ and $\boldsymbol{k}$ are orthogonal, in the direction of each coordinate axis we derive [17, 18]

$$\begin{aligned} \frac{\partial \sigma_{11}}{\partial x_1} + \frac{\partial \sigma_{12}}{\partial x_2} + \frac{\partial \sigma_{13}}{\partial x_3} + F_1 = 0, \\ \frac{\partial \sigma_{21}}{\partial x_1} + \frac{\partial \sigma_{22}}{\partial x_2} + \frac{\partial \sigma_{23}}{\partial x_3} + F_2 = 0, \\ \frac{\partial \sigma_{31}}{\partial x_1} + \frac{\partial \sigma_{32}}{\partial x_2} + \frac{\partial \sigma_{33}}{\partial x_3} + F_3 = 0 \end{aligned} \tag{2.4}$$

as the differential equations of equilibrium.

Sometimes it is necessary to use equilibrium equations (2.4) in the deformed configuration. Allthough in the reference configuration the body is referred to the Cartesian coordinate system, in the deformed configuration it is transformed into a curvilinear coordinate system, which is supposed to be orthogonal [17, 18]. Then, if the coordinate transformation is due to

$$\begin{pmatrix} \boldsymbol{i}' \\ \boldsymbol{j}' \\ \boldsymbol{k}' \end{pmatrix} = \begin{pmatrix} T_{11} & T_{12} & T_{13} \\ T_{21} & T_{22} & T_{23} \\ T_{31} & T_{32} & T_{33} \end{pmatrix} \begin{pmatrix} \boldsymbol{i} \\ \boldsymbol{j} \\ \boldsymbol{k} \end{pmatrix},$$

then from (2.4) we derive the equilibrium nonlinear equations in the deformed con-

figuration $\Omega^{\boldsymbol{\varphi}}$ [17, 18]

$$\begin{aligned}
&\frac{\partial}{\partial x_1}\left(\sigma_{11}T_{11}+\sigma_{12}T_{21}+\sigma_{13}T_{31}\right)+\frac{\partial}{\partial x_2}\left(\sigma_{12}T_{11}+\sigma_{22}T_{21}+\sigma_{23}T_{31}\right)+\\
&\qquad+\frac{\partial}{\partial x_3}\left(\sigma_{13}T_{11}+\sigma_{23}T_{21}+\sigma_{33}T_{31}\right)+F_1=0,\\
&\frac{\partial}{\partial x_1}\left(\sigma_{11}T_{12}+\sigma_{12}T_{22}+\sigma_{13}T_{32}\right)+\frac{\partial}{\partial x_2}\left(\sigma_{12}T_{12}+\sigma_{22}T_{22}+\sigma_{23}T_{32}\right)+\\
&\qquad+\frac{\partial}{\partial x_3}\left(\sigma_{13}T_{12}+\sigma_{23}T_{22}+\sigma_{33}T_{32}\right)+F_2=0,\\
&\frac{\partial}{\partial x_1}\left(\sigma_{11}T_{13}+\sigma_{12}T_{23}+\sigma_{13}T_{33}\right)+\frac{\partial}{\partial x_2}\left(\sigma_{12}T_{13}+\sigma_{22}T_{23}+\sigma_{23}T_{33}\right)+\\
&\qquad+\frac{\partial}{\partial x_3}\left(\sigma_{13}T_{13}+\sigma_{23}T_{23}+\sigma_{33}T_{33}\right)+F_3=0.
\end{aligned}\tag{2.5}$$

In order to establish a connection between the area element in the deformed and reference configurations, some relations between stress characteristic measures in both configurations are needed. Such a relation provides the so called Piola transform [18]. Let the deformation $\boldsymbol{\varphi}:\mathbb{R}^3\to\mathbb{R}^3$ from reference into deformed configuration be injective, i.e. the deformation gradient $\mathbf{F}=\nabla\boldsymbol{\varphi}$ is invertible everywhere in Ω. Then, for any tensor $\mathbf{T}$ defined in the reference configuration, Piola's transform puts the tensor $\mathbf{T}^{\boldsymbol{\varphi}}$ in correspondence , such that

$$\mathbf{T}\left(\boldsymbol{x}\right)=\mathbf{T}^{\boldsymbol{\varphi}}\left(\boldsymbol{x}^{\boldsymbol{\varphi}}\right)\operatorname{cof}\nabla\boldsymbol{\varphi}\left(\boldsymbol{x}\right),$$

where $\operatorname{cof}\mathbf{A}$ is the cofactor matrix of $\mathbf{A}$: $\operatorname{cof}\mathbf{A}=\mathbf{A}^{-\mathrm{T}}\det\mathbf{A}$.

If $\mathbf{T}^{\boldsymbol{\varphi}}$ denotes the Cauchy stress tensor in the deformed configuration, then $\mathbf{T}$ will denote the so called first Piola-Kirchhoff stress in the reference configuration. Evidently, it is non-symmetric. However, since the constitutive equations take simpler forms for symmetric stress tensors, the second Piola-Kirchhoff stress tensor is usually introduced according to

$$\boldsymbol{P}\left(\boldsymbol{x}\right)=\left(\nabla\boldsymbol{\varphi}\left(\boldsymbol{x}\right)\right)^{-1}\mathbf{T}^{\boldsymbol{\varphi}}\left(\boldsymbol{x}^{\boldsymbol{\varphi}}\right).$$

2.1.3 Constitutive Relations

In order to express the stress tensor components in terms of displacements, we also need relations between stress and strain tensor components. Such relations are often referred to as constitutive relations. In general, the constitutive relations for non-linear elastic materials are derived from the strain energy density by differentiating it with respect to strains (or equivalently stresses) [18]:

$$\boldsymbol{P}(\boldsymbol{\varepsilon}) = \frac{\partial W}{\partial \boldsymbol{\varepsilon}}, \tag{2.6}$$

or component-wise

$$\boldsymbol{P}_{ij}(\boldsymbol{\varepsilon}) = \frac{\partial W}{\partial \varepsilon_{ij}}, \tag{2.7}$$

where $W = W(\boldsymbol{\varepsilon})$ is the strain energy density. Since $\boldsymbol{\varepsilon}$ is symmetric, then (2.6) shows that, $\boldsymbol{P}$ is also symmetric.

Substituting (2.2) into (2.7), and resulting expressions into (2.5), differential equations in terms of displacements in the most general case are derived. By making assumptions of a particular structural theory, certain components of the above governing equations are simplified.

In particular, for linear elastic material [18]

$$W(\boldsymbol{\varepsilon}) = \frac{1}{2} C_{ijkl} \varepsilon_{ij} \varepsilon_{kl},$$

where C_{ijkl} are the material parameters, a direct stress therefore produces a proportional strain:

$$P_{ij}(\boldsymbol{\varepsilon}) = C_{ijkl} \varepsilon_{kl}. \tag{2.8}$$

(2.8) is often referred to as the generalized Hooke‘s law [17, 18].

2.1.4 Geometric and Material Nonlinearity, Linearization

Depending on the material, geometry, loading conditions, and so on, material and/or geometric nonlinear structural theories may be considered. Structural theories,

based on the general relations (2.1), are usually used to describe large displacements of structural elements and are often referred to as being geometrically non-linear. Structural theories, based on the general relations (2.6), are involved in studying structural elements of non-linear elastic materials, and are often referred to as physically non-linear.

Both material and geometric nonlinearities result in the presence of non-linear terms in governing equations, obtained from (2.5) which is extremely difficult, and at times even impossible, to solve analytically. Even though it makes the theoretical study of a model more realistic, it significantly complicates the structural analysis.

Nevertheless, in some specific cases, simplified structural theories may be considered which are less difficult to solve analytically or numerically. For example, if the amplitude of the resultant of external forces applied to the structure is small, then the term $\frac{\partial u_k}{\partial x_i}\frac{\partial u_k}{\partial x_j}$ in (2.1) is very small and can therefore be neglected. Furthermore, if the stress-strain relation for the material of a particular structure is close to linear, then as constitutive relations (2.8) can be considered. Structural mechanics completely based on linear relations (2.3) and (2.8) is often called linear theory of structural mechanics.

2.2 Euler-Bernoulli Beam Structure

Beams are one of the simplest structural elements. Beams are structures where two of the dimensions are considerably smaller than the third one. In general, beams are subjected to lateral loads. Several beam theories have been developed based on various assumptions, and have therefore led to different levels of model accuracy. Evidently, depending on the problem under consideration, different groups of assumptions may be considered to construct a proper structural theory. One of the main structural theories for beams is the Euler-Bernoulli theory, which is based on the assumptions [14, 18, 22]:

i) the cross-section of the beam is infinitely rigid (undeformable) in its own plane,

ii) the cross-section of the beam remains plane after deformation,

iii) the cross-section remains normal to the deformed axis of the beam.

Based on those assumptions, the in-plane displacement field of the beam is represented by two rigid body translations and one rigid body rotation [22]. In terms of the displacements, for a straight plane beam, positioned on x-axis, the Euler-Bernoulli assumptions simply mean [38]

$$u_1 = u(x) - z\phi\,(x)\,,\ u_2 = 0,\ u_3 = w(x). \tag{2.9}$$

Experimental measurements show that these assumptions are valid for long, slender beams made of isotropic materials with solid cross-sections [22]. When one or more of these conditions are not met, Euler-Bernoulli beam theory predictions can become inaccurate.

In Figure 2.1 the differential element dx of a beam subject to some arbitrary loadings p and q is shown.

In this case, the kinematic relations are

$$\varepsilon = \lambda - 1, \quad \phi = \arctan\frac{w'}{1+u'}, \quad \kappa = \phi', \tag{2.10}$$

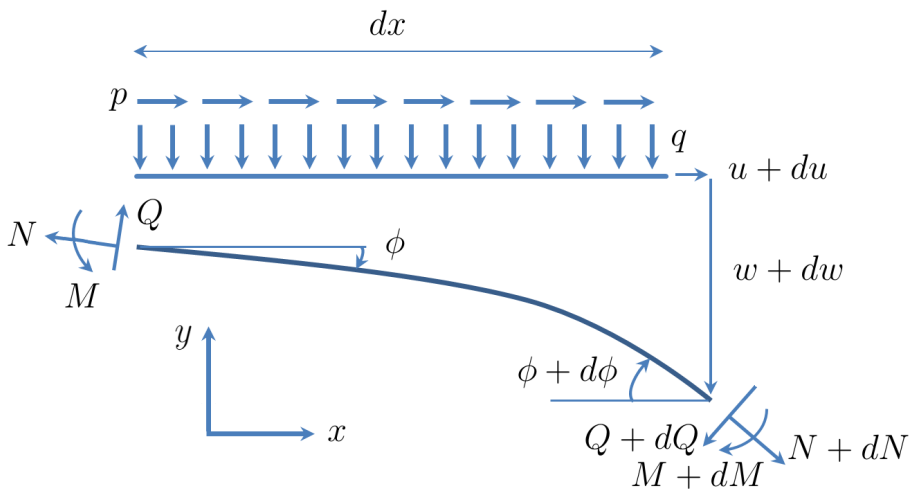

Figure 2.1: Equilibrium of the beam in the deformed configuration

where $\lambda = \sqrt{(1+u')^2 + (w')^2}$, to which the equilibrium equations

$$\begin{gathered}(N \cdot \cos\phi - Q \cdot \sin\phi)' + p = 0, \quad (N \cdot \sin\phi + Q \cdot \cos\phi)' + q = 0, \\ M' - \lambda \cdot Q = 0,\end{gathered} \tag{2.11}$$

and the material laws

$$N = EA \cdot \varepsilon, \quad M = -EJ \cdot \kappa, \tag{2.12}$$

must be added to obtain a full system. Using Taylor series expansion for nonlinear terms in (2.10)–(2.12), three theories are derived, referred to as first, second and third order theories [12, 13, 35, 48].

Considering the Taylor series expansions

$$\cos\phi\big|_{\phi=0} \approx 1 + \mathcal{O}(2),$$

$$\sin\phi\big|_{\phi=0} \approx \phi + \mathcal{O}(2),$$

$$\arctan\frac{w'}{1+u'}\bigg|_{w'=0,u'=0} \approx w'(1-u') + \mathcal{O}(3),$$

$$[\lambda - 1]\,\big|_{w'=0,u'=0} \approx u' + \frac{1}{2}(w')^2\left[1 - u' + (u')^2\right] + \mathcal{O}(3),$$

$$\left.\frac{1}{\lambda}\right|_{w'=0,u'=0} \approx 1 - u' + \mathcal{O}(2),$$

where $\mathrm{O}(k)$, $k = 2, 3$, stands for k^{th} order terms, in the first order theory from (2.10), (2.11), it is obtained respectively:

$$\varepsilon = u', \quad \phi = w', \quad \kappa = \phi', \tag{2.13}$$

$$N + p = 0, \quad Q' + q = 0, \quad Q - M' = 0. \tag{2.14}$$

Consequently, we arrive at the following system of two uncoupled ODE's:

$$\begin{aligned} (EAu')' &= -p(x), \\ (EIw'')'' &= q(x), \quad 0 < x < l. \end{aligned} \tag{2.15}$$

This means, that both equations can be solved for u and w separately. If the beam is homogeneous, and its cross-section is of constant axial stiffness EA and bending stiffness EJ, then from (2.15) we derive

$$\begin{aligned} EAu'' &= -p(x), \\ EIw'''' &= q(x), \quad 0 < x < l. \end{aligned} \tag{2.16}$$

The second–order theory is based on the same kinematic relations as the first–order theory, whereas the second equilibrium equation of (2.11) is substituted by

$$(Nw')' + Q' + q = 0,$$

and the consequent system of equations is of the form

$$\begin{aligned} (EAu')' &= -p(x), \\ (EIw'')'' - (EAu'w')' &= q(x), \end{aligned} \quad 0 < x < l. \tag{2.17}$$

Evidently, u' can be determined independently from the first equation and substituted into the second one, which can then be merely expressed in terms of w.

The third order theory is based on nonlinear kinematic relations

$$\varepsilon = u' + \frac{1}{2}\left(w'\right)^2, \quad \phi = w'\left(1 - u'\right),$$

and equilibrium equations

$$N + p = 0, \quad \left(Nw'\right)' + Q' + q = 0, \quad Q - \left(1 - u'\right)M' = 0.$$

The consequent system of equations is of the form

$$\begin{aligned}
&\left[EA\left(u' + \frac{1}{2}\left(w'\right)^2\right)\right]' - \left[\left(EI\left[\left(u'w'\right)' - w''\right]\right)' w'\right]' = p(x), \\
&\left(EI\left[\left(u'w'\right)' - w''\right]\right)'' + \left(EI\left[\left(u'w'\right)' - w''\right]\right)' u' - \\
&- \left[EA\left(u' + \frac{1}{2}\left(w'\right)^2\right) w'\right]' = q(x), \\
&\qquad\qquad 0 < x < l.
\end{aligned} \tag{2.18}$$

System (2.18) is a fully coupled system of nonlinear ODE's.

Chapter 3

Finite Element Method

Finite element methods divide the reference configuration of the structure under analysis into smaller parts of basic geometry called elements. They derive equilibrium equations for typical elements and then use appropriate variational methods to find the approximate solution for the problem by minimizing some error functional . Division into smaller elements overcomes difficulties such as complex geometry, local effects or material non-homogeneity.

In this chapter we summarize the main concepts for finite element technique which aims to find approximate solutions for boundary value problems expressed by differential equations in ordinary derivatives. After a short introduction to FEM, some known weighted residual methods are described.

Finite element discretization is demonstrated for geometrically linear and non-linear structural theories for beams. The discretized linear systems of algebraic equations are derived in both linear and non-linear theories.

The material is mainly based on [14, 38].

3.1 Introduction

Analysis of structural elements (rods, beams, frames, plates, shells, etc.) is equivalent to the solution of differential equations under appropriate loading and boundary conditions. FE consists of two main steps – discretization and approximation. Discretization is a procedure whereby the domain of the reference configuration is divided into small sub-domains of simple geometry, called *finite elements*. Approximation mainly includes two steps:

i) the unknown field quantities are expanded into a finite sum of specific polynomials or *basis functions*, weighted by expansion coefficients which are to be determined for each sub-domain,

ii) algebraic relations or *element equations* derived for the expansion coefficients are gathered using continuity conditions for neighbouring elements.

The expansion coefficients are often associated with the solution value at the nodes.

The approximate solution of static problem for a beam is represented as follows [14, 38]

$$w_N(x) = \sum_{n=1}^{N} \alpha_n \psi_n(x), \quad x \in [0, l], \tag{3.1}$$

in which ψ_n are the linearly independent basis functions and $\alpha_n \in \mathbb{R}$ are the expansion coefficients (the values of w_N at discretization nodes), N is the DOF of the FE model.

FEM has several advantages, among which are much freedom in the choice of discretization, i.e. the type and number of elements used to discretize the domain, choice of order of continuity of the basis functions and efficiency for problems defined with complicated geometry, etc.

3.2 Weighted Residual Method

There are several approaches to determine the expansion coefficients α_n, $n = 1, \ldots, N$ in (3.1). Suppose that, the governing equation has the general form

$$\mathcal{D}[w] = f \quad \text{in } \Omega, \tag{3.2}$$

where $\Omega \subset \mathbb{R}^3$ is an open domain, subject to the boundary conditions

$$\mathcal{B}[w] = w_b \quad \text{on } \partial\Omega. \tag{3.3}$$

Above $\mathcal{D}[\cdot]$ is a differential operator, $\mathcal{B}[\cdot]$ is the operator of boundary conditions.

Assume, that the basis functions ψ_n in (3.1) satisfy boundary conditions (3.3). Then, in general, (3.1) does not satisfy (3.2) exactly, in the sense that, in general, the residual

$$\mathcal{R}_N := \mathcal{D}[w_N] - f \not\equiv 0 \quad \text{a.e. in } \Omega. \tag{3.4}$$

If apparently for some choice of α_n and ψ_n, $\mathcal{R}_N \equiv 0$ throughout the domain, then w_N is the solution of (3.2).

Weighted residual methods [14, 38] provide exactly N equations expressed as

$$\int_\Omega \mathcal{R}_N(\boldsymbol{x})\, \rho_n(\boldsymbol{x})\, d\boldsymbol{x} = 0, \quad n = 1, \ldots, N, \tag{3.5}$$

in which ρ_n are so-called weight functions, supposed to be non-zero and linearly independent. Evidently, a different choice of weight functions will result in different discrete equations.

One of the usual weighted residual methods is the least square approach, i.e. α_n, $n = 1, \ldots, N$, are chosen to minimize the functional [14]

$$\Phi[\alpha_N] = \int_\Omega \mathcal{R}_N^2(\boldsymbol{x})\, d\boldsymbol{x}. \tag{3.6}$$

A system of equations for the coefficients α_n is obtained via

$$\frac{\partial \Phi}{\partial \alpha_n} = 0, \quad n = 1, \ldots, N. \tag{3.7}$$

Another approach is the Galerkin (known also as Bubnov–Galerkin) method, which is used to determine the expansion coefficients from the following set of equations [14, 38]:

$$\int_{\Omega} \mathcal{R}_N(\boldsymbol{x})\, \psi_n(\boldsymbol{x})\, d\boldsymbol{x} = 0, \quad n = 1, \ldots, N, \tag{3.8}$$

i.e. $\rho_n = \psi_n$.

Weighted residuals methods differ from each other in the choice of weight function ρ. Ultimately, weighted residual methods reduce the original problem to a system of the form [14, 38]

$$\mathbf{K}(\boldsymbol{\alpha})\, \boldsymbol{\alpha} = \boldsymbol{f}, \tag{3.9}$$

for unknowns $\boldsymbol{\alpha} = (\alpha_1 \;\; \alpha_2 \;\; \ldots \;\; \alpha_N)^T$ and determined $\mathbf{K} \in \mathbb{R}^{N \times N}$ and $\boldsymbol{f} \in \mathbb{R}^N$. Different methods lead to different $\mathbf{K}$ and $\boldsymbol{f}$. If the differential operator $\mathcal{D}$ is linear, then $\mathbf{K}$ does not depend on $\boldsymbol{\alpha}$.

3.2.1 Weak Formulation

Direct or differential formulation of the problem in the form of (3.2), (3.3) imposes certain smoothness requirements on the right hand side for its traditional solution to exist. Consideration of the so-called weak or variational formulation of the problem makes it possible to lower such requirements.

It is usually formed by multiplying the governing system (3.2) by some, appropriately chosen test function and integrating over the whole domain [14]:

$$\int_{\Omega} \mathcal{D}[w]\, \varphi(\boldsymbol{x})\, d\boldsymbol{x} - \int_{\Omega} f(\boldsymbol{x})\, \varphi(\boldsymbol{x})\, d\boldsymbol{x} = 0. \tag{3.10}$$

Eq. (3.10) is called the integral formulation of (3.2). Integrating the first term of (3.10) by parts, the boundary conditions are included in it, leading to the weak formulation of the problem.

3.2.2 Treatment of Non-Linearities in the Weak Form

All types of non-linearities, i.e. physical (material), geometric, force, etc., can be included in the weak form of static problem formulation by directly using the strong form equilibrium equations:

$$\frac{\partial \sigma_{ij}}{\partial x_j} + f_i = 0 \quad \text{in} \quad \Omega, \tag{3.11}$$

subjected to boundary conditions

$$\sigma_{ij} n_j = b_i \quad \text{on} \quad \partial\Omega.$$

Multiplying both sides of (3.11) by some smooth function $\varphi \in C_0^\infty(\Omega)$, and integrating by parts, we will arrive at the weak formulation of the problem in stress tensor components

$$\int_\Omega \sigma_{ij} \frac{\partial \varphi_i}{\partial x_j} d\boldsymbol{x} = \int_{\partial\Omega} b_i \varphi_i ds + \int_\Omega f_i \varphi_i d\boldsymbol{x}. \tag{3.12}$$

If it is assumed that material non-linearity is in the form of (2.6), then (3.12) will become [39]

$$\int_\Omega \sigma_{ij}(\boldsymbol{\varepsilon}) \frac{\partial \varphi_i}{\partial x_j} d\boldsymbol{x} = \int_{\partial\Omega} b_i \varphi_i ds + \int_\Omega f_i \varphi_i d\boldsymbol{x}. \tag{3.13}$$

Thus, even in the case of infinitesimal strains (2.3), (3.13) is a nonlinear constraint with respect to displacement vector $\boldsymbol{u}$:

$$\int_\Omega \sigma_{ij} \left(\nabla \boldsymbol{u} + (\nabla \boldsymbol{u})^T \right) \frac{\partial \varphi_i}{\partial x_j} d\boldsymbol{x} = \int_{\partial\Omega} b_i \varphi_i ds + \int_\Omega f_i \varphi_i d\boldsymbol{x}. \tag{3.14}$$

Furthermore, if it is assumed that the body is isotropic, i.e. the stress tensor depends on strain tensor linearly or (2.8) holds, but the strain tensor is given in the form (2.1), then (3.12) yields [2, 39]

$$\frac{1}{2} \int_\Omega C_{ijkl} \left[\frac{\partial u_k}{\partial x_l} + \frac{\partial u_l}{\partial x_k} + \frac{\partial u_m}{\partial x_k} \frac{\partial u_m}{\partial x_k} \right] \frac{\partial \varphi_i}{\partial x_j} d\boldsymbol{x} = \int_{\partial\Omega} b_i \varphi_i ds + \int_\Omega f_i \varphi_i d\boldsymbol{x}. \tag{3.15}$$

Eq. (3.15) is nonlinear with respect to the displacement vector components u_i.

3.2.2.1 Linearization

Accounting for non-linearities, like material or geometrical, as shown above, reduces (3.14) and (3.15) to (3.9) with $\mathbf{K} = \mathbf{K}(\boldsymbol{\alpha})$. Depending on the form of $\mathbf{K} = \mathbf{K}(\boldsymbol{\alpha})$, the determination of $\boldsymbol{\alpha}$ can be significantly complicated. The linearization of $\mathbf{K}$ is one way for overcoming this. For instance, in (3.14), the material non-linearity functions ς_{ij} are usually expanded into Taylor series and the first, linear term is considered. As a result instead of (3.9) we obtain a simpler system

$$\mathbf{K}_{lin}\boldsymbol{\alpha} = \boldsymbol{b}, \tag{3.16}$$

which can be solved using efficient numerical methods for linear systems.

3.2.2.2 Newton-Raphson Method

An iterative method of determining $\boldsymbol{\alpha}$ from (3.9) is the Newton-Raphson method of finding the roots of non-linear algebraic equations [39]. The iterative algorithm is based on Taylor series expansion of (3.9) near prescribed state $\boldsymbol{\alpha}_i$.

For (3.9) at i-th iteration step, $i = 0, 1, \ldots,$ we have

$$\mathbf{K}(\boldsymbol{\alpha}_i + d\boldsymbol{\alpha}_i)\left(\boldsymbol{\alpha}_i + d\boldsymbol{\alpha}_i\right) - \boldsymbol{b} = \mathbf{K}(\boldsymbol{\alpha}_i)\boldsymbol{\alpha}_i - \boldsymbol{b} + \mathbf{J}\left(\boldsymbol{\alpha}_i\right) \cdot d\boldsymbol{\alpha}_i + \mathrm{O}\left(d\boldsymbol{\alpha}_i^2\right), \tag{3.17}$$

in which $d\boldsymbol{\alpha}_i$ is usually called solution increment, $\mathbf{J}\left(\boldsymbol{\alpha}_i\right) = \nabla\mathbf{K}\left(\boldsymbol{\alpha}_i\right)$ is the Jacobian matrix. In each single step the residual

$$\boldsymbol{r}_i = \boldsymbol{b} - \mathbf{K}(\boldsymbol{\alpha}_i)\boldsymbol{\alpha}_i,$$

and the solution increment must be computed

$$d\boldsymbol{\alpha}_i = \mathbf{J}^{-1}(\boldsymbol{\alpha}_i)\boldsymbol{r}_i.$$

Eventually, the updated solution will be

$$\boldsymbol{\alpha}_{i+1} = \boldsymbol{\alpha}_i + d\boldsymbol{\alpha}.$$

The iterative procedure stops when $d\boldsymbol{\alpha}_i$ and $\boldsymbol{r}_i$ have reached a required tolerance. The convergence rate of the algorithm is expressed via

$$||\boldsymbol{\alpha}_{i+1} - \boldsymbol{\alpha}|| \leq C \, ||\boldsymbol{\alpha}_i - \boldsymbol{\alpha}||^2 ,$$

where C is some constant, independent on $\boldsymbol{\alpha}$.

3.3 Finite Element Method for Structures

In this section the main FEM characteristics for Euler-Bernoulli (one-dimensional) theory are represented.

3.3.1 FEM for Euler-Bernoulli Beam: Geometrically Linear Theory

Euler-Bernoulli beam theories are introduced in Section 2.2. Using the expressions for stresses and strains within first-, second- and third-order theories, weak formulations for the corresponding theories are introduced in this section. Multiplying (2.14) by virtual displacements in axial and normal directions, the following is obtained:

$$\int [N' + p_x]\delta u dx + \int [M'' + p_z]\delta w dx = 0.$$

Integrating by parts, the following is obtained

$$-\int N\delta u' dx + \int M\delta w'' dx + \int p_x \delta u dx + \int p_z \delta w dx = 0.$$

Here and in what follows, the boundary terms, resulting from integration by parts, are neglected.

Taking into account, that within first order theory

$$\delta\varepsilon = \delta u', \quad \delta\kappa = \delta w'',$$

the last equality reads as

$$\int N\delta\varepsilon dx - \int M\delta\kappa dx = \int p_x \delta u dx + \int p_z \delta w dx.$$

On the other hand,

$$N = EA\varepsilon_{lin}, \quad M = -EJ\kappa,$$

therefore, finally,

$$\int EA\varepsilon_{lin}\delta\varepsilon dx + \int EJ\kappa\delta\kappa dx = \int p_x \delta u dx + \int p_z \delta w dx. \tag{3.18}$$

Here ε_{lin} is the linearized strain.

Applying the Newton-Raphson procedure to the left hand side of (3.18):

$$\int EA\varepsilon_{lin}\delta\varepsilon dx + \int EJ\kappa\delta\kappa dx = \int EA\Delta\varepsilon_{lin}\delta\varepsilon dx + \int EA\varepsilon_{lin}\Delta\delta\varepsilon dx +$$
$$+ \int EJ\Delta\kappa\delta\kappa dx + \int EJ\kappa\Delta\delta\kappa dx,$$

which can be simplified further taking into account, that in the first order theory

$$\Delta\varepsilon_{lin} = \Delta u', \quad \Delta\kappa = \Delta w'', \quad \Delta\delta\varepsilon = \Delta\delta\kappa = 0.$$

Finally, for tangent and current stiffnesses, the following is obtained

$$J(x) = \int EA\Delta u'\delta u' dx + \int EJ\Delta w''\delta w'' dx$$

and

$$A(x) = \int EAu'\delta u' dx + \int EJw''\delta w'' dx.$$

3.3.2 FEM for Euler-Bernoulli Beam: Geometrically Nonlinear Theory

The second order theory is now considered, where it is assumed, that the geometric relation between strain and displacements is nonlinear:

$$\varepsilon = u' + \frac{1}{2}w'.$$

Then, similar to (3.18), in this case

$$\int EA\varepsilon_{lin}\delta\varepsilon dx + \int EJ\kappa\delta\kappa dx = \int p_x\delta u dx + \int p_z\delta w dx,$$

where

$$\delta\varepsilon = \delta u' + w'\delta w'.$$

In this case the Newton-Raphson procedure leads to

$$\int EA\varepsilon_{lin}\delta\varepsilon dx + \int EJ\kappa\delta\kappa dx = \int EA\Delta\varepsilon_{lin}\delta\varepsilon dx +$$

$$+\int EA\varepsilon_{lin}\Delta\delta\varepsilon dx+\int EJ\Delta\kappa\delta\kappa dx+\int EJ\kappa\Delta\delta\kappa dx$$

with

$$\Delta\varepsilon_{lin}=\Delta u',\quad \Delta\kappa=\Delta w'',\quad \Delta\delta\varepsilon=\delta w'\cdot\Delta w',\quad \Delta\delta\kappa=0.$$

Therefore, the tangent and current stiffnesses are as follows:

$$J(x)=\int EA\Delta u'\left(\delta u'+w'\delta w'\right)dx+\int EAu'\delta w'\cdot\Delta w'dx+\int EJ\Delta w''\delta w''dx,$$

and

$$A(x)=\int EAu'\left(\delta u'+w'\delta w'\right)dx+\int EJw''\delta w''dx.$$

Based on the assumptions of the third order theory, the following is derived:

$$\int EA\varepsilon\delta\varepsilon dx+\int EJ\kappa\delta\kappa dx=\int p_x\delta udx+\int p_z\delta wdx.$$

In this case, the Newton-Raphson procedure provides

$$\int EA\varepsilon\delta\varepsilon dx+\int EJ\kappa\delta\kappa dx=\int EA\Delta\varepsilon\delta\varepsilon dx+$$

$$+\int EA\varepsilon\Delta\delta\varepsilon dx+\int EJ\Delta\kappa\delta\kappa dx+\int EJ\kappa\Delta\delta\kappa dx$$

with

$$\Delta\varepsilon=\Delta u'+w'\cdot\Delta w',\quad \Delta\kappa=\Delta w'',\quad \Delta\delta\varepsilon=\delta w'\cdot\Delta w',\quad \Delta\delta\kappa=0.$$

Therefore, the tangent and current stiffnesses are defined through:

$$J(x)=\int EA\left(\Delta u'+w'\cdot\Delta w'\right)\left(\delta u'+w'\delta w'\right)dx+$$

$$+\int EA\left(u'+\frac{1}{2}\left(w'\right)^2\right)\delta w'\cdot\Delta w'+\int EJ\Delta w''\delta w''dx$$

and

$$A(x)=\int EA\left(u'+\frac{1}{2}\left(w'\right)^2\right)\left(\delta u'+w'\cdot\delta w'\right)dx+\int EJw''\delta w''dx.$$

3.4 Error Measures

In general, the approximate solution obtained with FEM may contain three types of errors:

1. domain approximation or division into finite elements,
2. numerical (mainly due to intermediate computations and integral evaluations),
3. solution approximation (cf. (3.1)).

The first type makes sense in the discretization of domains with complex and irregular geometry and can therefore be improved by refining the mesh. The second type of errors depends mainly on the total degrees of freedom, and therefore makes sense when greater accuracy is required. The third type of errors always exists and can be improved by increasing N or the polynomial order of the ansatz functions.

The efficiency of the FE solution is measured by the error between analytical and approximate solutions. There are several ways to measure this error. Examples include C norm

$$||w - w_N||_C = \max_{\boldsymbol{x}\in\Omega} |w(\boldsymbol{x}) - w_N(\boldsymbol{x})|\,,$$

L^2 norm

$$||w - w_N||_{L^2} = \left[\int_\Omega |w - w_N|^2\, d\boldsymbol{x}\right]^{1/2},$$

$W^{1,2}$ norm

$$||w - w_N||_{W^{1,2}} = \left[\int_\Omega |w' - w'_N|^2\, d\boldsymbol{x} + \int_\Omega |w - w_N|^2\, d\boldsymbol{x}\right]^{1/2},$$

etc. The approximate solution (3.1) converges to the analytical solution, if [14]

$$||w - w_N|| \leq ch^p,$$

for some positive constant c independent of both solutions and convergence rate $p > 0$, h is the characteristic length of the element.

Chapter 4

Model Order Reduction

It is relatively recent that model order reduction or MOR methods have been applied to statics of structures. The need to develop reliable reduction techniques for structural analysis of static systems was overlooked, the reasoning being that high computational efforts were not required to solve such problems and that reduction techniques can reduce the order of the problem, but not necessarily computational time and costs. As already mentioned in the Introduction, model order reduction for the analysis of statics of structures becomes meaningful only when used for repetitive calclations, which are part of design verification analysis.

In this Chapter we will take a closer look at the general principles of the model order reduction method. The projection procedure is explained; and methods to construct suitable projection bases are also developed. Assuming that as a result of discretization, the following parametrized system is obtained:

$$\mathbf{K}(\boldsymbol{\mu}, \boldsymbol{\alpha})\, \boldsymbol{\alpha}(\boldsymbol{\mu}) = \boldsymbol{b}(\boldsymbol{\mu}), \tag{4.1}$$

in which $\boldsymbol{\mu} \in \mathbb{R}^n$ is the vector of parameters. It involves n degrees of freedom. The aim is to approximate this system by a much smaller system using only $k \ll n$ degrees of freedom. To this end, a new k dimensional subspace is built, into which the original system is projected. The projection means that the residue of the

original system must be orthogonal to the basis $\mathbf{W} \in \mathbb{R}^{n \times k}$ of the new subspace. The vector of unknowns $\boldsymbol{\alpha} \in \mathbb{R}^n$ is substituted by a new vector $\overline{\boldsymbol{\alpha}} \in \mathbb{R}^k$ defined through $\mathbf{W}^{\mathrm{T}}$. After this, using the matrix multiplication rule, the following reduced order system is derived

$$\overline{\mathbf{K}}\left(\boldsymbol{\mu}, \overline{\boldsymbol{\alpha}}\right) \overline{\boldsymbol{\alpha}}\left(\boldsymbol{\mu}\right) = \overline{\boldsymbol{b}}\left(\boldsymbol{\mu}\right), \tag{4.2}$$

which involves less degrees of freedom in $\overline{\boldsymbol{\alpha}} \in \mathbb{R}^k$.

By solving (4.1) with respect to $\boldsymbol{\alpha}$ for different values of $\boldsymbol{\mu}$, we eventually obtain the set of vectors $\mathbf{A} = \{\boldsymbol{\alpha}\left(\mu_1\right), \ldots, \boldsymbol{\alpha}\left(\mu_k\right)\} := \{\boldsymbol{\alpha}_1, \ldots, \boldsymbol{\alpha}_k\}$. It is this set of so-called snapshots which is used in POD based MOR methods (see Chapter 1). The required data can also be obtained without any significant difficulty by means of sensors and transducers through experiments that are performed repeatedly during design verification.

The process of obtaining these snapshots by varying the value of the parameter is called the *offline phase*. The snapshots may be used to construct various subspaces, into which the initial system may be projected. This step of the reduction is called the *online phase*.

The reduction is in the choice of a proper $k-$ dimensional subspace with an orthonormal basis $\mathbf{W} = \{\boldsymbol{w}_1, \ldots, \boldsymbol{w}_k\}$ and the solution of the problem in it. Now, the aim is to find an appropriate $\boldsymbol{w} \in \mathbf{W}$, which approximates $\boldsymbol{\alpha}$ in some sense. The most common ways include:

1. The Ritz-Galerkin approach, which requires that the residual $\boldsymbol{b} - \mathbf{K}\boldsymbol{w}$ is orthogonal to $\mathbf{W}$.

2. The minimum norm residual approach, which requires that the Euclidean norm $||\boldsymbol{b} - \mathbf{K}\boldsymbol{w}||^2$ is minimal over $\mathbf{W}$.

3. The Petrov-Galerkin approach, which requires that the residual $\boldsymbol{b} - \mathbf{K}\boldsymbol{w}$ is orthogonal to some other suitable $k-$dimensional subspace.

4. The minimum norm error approach, which requires that the Euclidean norm $||\boldsymbol{w} - \boldsymbol{\alpha}||^2$ is minimal.

The Ritz-Galerkin projection approach is used here according to which the new subspace should be orthogonal to the residual:

$$\mathbf{W}^T \left[\mathbf{K}\left(\boldsymbol{\mu}, \boldsymbol{\alpha}\right) \boldsymbol{\alpha}\left(\boldsymbol{\mu}\right) - \boldsymbol{b}\left(\boldsymbol{\mu}\right)\right] = 0. \tag{4.3}$$

Its solution $\boldsymbol{\alpha}$ can be represented in the new subspace as $\boldsymbol{\alpha} = \mathbf{W}\overline{\boldsymbol{\alpha}}$:

$$\mathbf{W}^T \mathbf{K}\left(\boldsymbol{\mu}, \boldsymbol{\alpha}\right) \mathbf{W}\overline{\boldsymbol{\alpha}}\left(\boldsymbol{\mu}\right) - \mathbf{W}^T \boldsymbol{b}\left(\boldsymbol{\mu}\right) = 0, \tag{4.4}$$

or

$$\mathbf{W}^T \mathbf{K}\left(\boldsymbol{\mu}, \boldsymbol{\alpha}\right) \mathbf{W}\overline{\boldsymbol{\alpha}}\left(\boldsymbol{\mu}\right) = \mathbf{W}^T \boldsymbol{b}\left(\boldsymbol{\mu}\right), \tag{4.5}$$

After some denotations the reduced system (4.2) will be obtained. From now on, the most important aspect is the proper choice of the basis $\mathbf{W}$.

4.1 MOR for Linear Systems

In this section some methods used to construct suitable projection bases to perform order reduction for linear systems are reviewed.

4.1.1 Krylov Subspace

Krylov subspaces are constructed in the usual way, and are described in the corresponding subsection in the Introduction (cf. (1.2.1.1)). In dynamic problems, the starting vector $\boldsymbol{v}$, spanning the Krylov subspace, is just a vector with $||\boldsymbol{v}|| = 1$, and more often it is chosen to be $\boldsymbol{v} = \boldsymbol{b}/\,||\boldsymbol{b}||$.

To span a Krylov subspace providing reduced solution for structural analysis of static systems one (any) of the snapshots is chosen. The vectors generated based on that snapshot are then QR-factorized to be orthonormalized:

$$\left\{\boldsymbol{\alpha}_1, \mathbf{K}\boldsymbol{\alpha}_1, \mathbf{K}^2\boldsymbol{\alpha}_1, \ldots, \mathbf{K}^k\boldsymbol{\alpha}_1\right\} = \mathbf{QR}. \tag{4.6}$$

This basis is used to project the matrix $\mathbf{K}$ into the constructed subspace.

Solving the reduced system and then projecting the solution vector back to the large space, the solution obtained of the large system is $\boldsymbol{\alpha}$.

The disadvantage of this method is costly computation of powers of discretization matrix $\mathbf{K}$. On the other hand, it only uses one snapshot to construct the projection subspace, which is a clear advantage when, for example, previously performed experiments fail to provide much information for the new area of interest and analysis. In this case, the computation of powers of $\mathbf{K}$ is more efficient, than performing a new experiment.

4.1.2 Inexact Krylov Subspace

Inexact Krylov is a new type of a subspace, which is constructed using several/a few snapshots. The subspace is defined by (cf. (1.2.1.1))

$$\mathbf{Kr}\left(\mathbf{K};\boldsymbol{\alpha}\right)=\text{span}\left\{\boldsymbol{\alpha}_1,\mathbf{K}\boldsymbol{\alpha}_1,\ldots,\boldsymbol{\alpha}_k,\mathbf{K}\boldsymbol{\alpha}_k\right\},\quad k<n.$$

The further algorithm is the same as in Subsection 4.1.1. The advantage of the inexact Krylov subspace method, compared with the previous one, is that here there is no need to compute any power of the stiffness matrix $\mathbf{K}$.

4.1.3 Full Basis Subspace

The full set of snapshots is used as the basis to construct a new type of projecting subspace. They are first orthonormalized:

$$\left\{\boldsymbol{\alpha}_1,\ldots,\boldsymbol{\alpha}_k\right\}=\mathbf{QR}. \tag{4.7}$$

And then the procedure that follows is the same as above. Computationally, this is the most efficient method. However, it requires more snapshots than the previous methods and sometimes they can be impossible to obtain, for example, for analysis of areas where sensors cannot be installed.

4.2 MOR for Nonlinear Systems

In non-linear problems the stiffness matrix is not constant and changes along the equilibrium path. To overcome this difficulty, Newton-Raphson iteration is used (see Paragraph 3.2.2.2), In Figure 4.1 the scheme of Newton-Raphson iteration on the equilibrium path is illustrated, where ΔF and ΔU are the force and displacement increments at each iteration step, respectively. At each iteration step $\mathbf{K}$ is constant, which means it is possible to consider a non-linear problem as a set of linear problems. Therefore, by using one of the aforementioned MOR methods (see Section 4.1), a linear problem is reduced instead of solving the higher fidelity problem. A smaller system is solved and that solution is used as an increment for the next iteration step. This procedure ends when the solution converges.

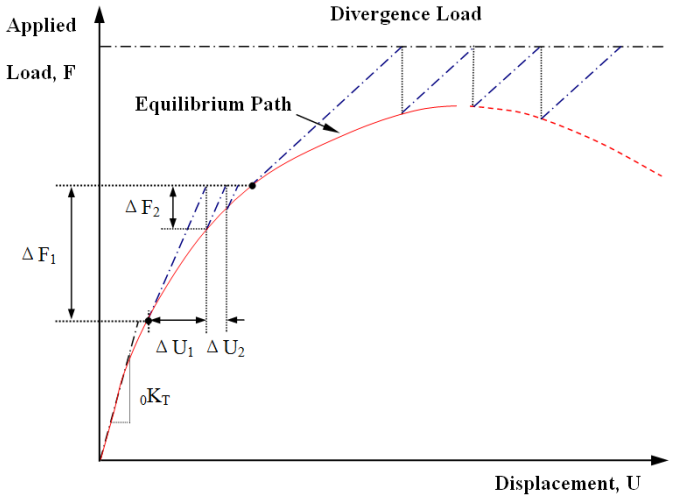

Figure 4.1: Newton-Raphson iteration diagram

The offline procedure seems costly, but in industry non-linear analysis is very often carried out as "real life" Newton-Raphson iteration. For each load step, sensors can provide the data to construct projection bases and reduce subspaces.

Chapter 5

Application to Model Problems and Evaluation

To verify the efficiency of each of the MOR techniques discussed in Chapter 4, several model problems are considered and corresponding error estimations are carried out. To prove the flexibility of these methods, different types of structures are considered: a simple cantilever beam; a beam structure consisting of 2 beams connected to each other with a joint; and a simple frame structure. The analytical solution for these systems for first- and second-order theories are also calculated to show the difference in the system's behaviour when using linear and non-linear theories. All exemplary problems are parametrized by localization of the external loading. The approximate FE solution for different values of the parameter is computed and the so-called snapshots are collected. In the MOR application step, different locations are chosen for the external loading and previously obtained snapshots are used to construct the projection subspaces using the three different techniques described in Chapter 4.

Discretization of the differential equations is carried out using linear or non-linear FEM depending on the theory involved. (The calculations are carried out in Python solver.)

5.1 Exemplary Problems

Rigorous solutions are obtained only in the framework of the first- and second-order theories, since in these cases the governing systems are linear (see Section 2.2 for details). Approximate solutions for all exemplary problems in terms of the third-order theory are obtained using FEM.

5.1.1 First Exemplary Problem

Consider a simple horizontal cantilever beam subjected to longitudinal H and transverse P constant forces at $x = l_1$ end of the beam (see Figure 5.1).

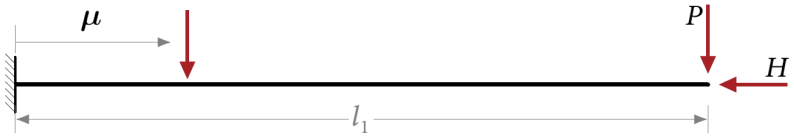

Figure 5.1: Simple cantilever beam: First exemplary problem

5.1.1.1 Exact solution

The input parameters are chosen to be $P = 0.1$ N, $H = 1$ N, $A = 10^{-4}$ m^2, $I_y = 10^{-9}$ m^4, $E = 2 \cdot 10^8$ N/m^2.

i) First order theory:

In the geometrically linear case the equilibrium is stated using the undeformed configuration of the beam. Longitudinal force H shows only compression effect.

The displacements of the beam are given by

$$\begin{aligned} u(x) &= \frac{Hx}{EA}, \\ w(x) &= \frac{Px^2(x - 3l_1)}{6EI}, \end{aligned} \qquad 0 \le x \le l_1. \tag{5.1}$$

ii) Second order theory:

In the geometrically non-linear case, the equilibrium is stated using the deformed configuration of the beam. For the particular exemplary problem this results in bending moment. Normal force H is assumed to remain constant along the beam and contributes an additional moment which depends on the actual deformation w of the beam in the current configuration.

The displacement of the beam is given by

$$\begin{aligned} u(x) &= \frac{H}{EA}x, \\ w(x) &= -\frac{P}{Hk}\left[kx - \sin(kx) - \tan(kl)[\cos(kx) - 1]\right], \end{aligned} \qquad 0 \le x \le l_1, \tag{5.2}$$

where

$$k^2 = \frac{H}{EI}.$$

In order to study the dependence of the value of the horizontal force H the first- and second-order theories, the critical value of the horizontal buckling load has first to be determined. For chosen parameters it is computed to be $H \approx 1.97192$. In order to visualise the difference between the first- and second-order theories in this particular example, depending on the value of the horizontal force, the transverse displacement of the beam, $w(x)$, from (5.1) and (5.2) is plotted at $x = l_1$ when H is in the range of the precritical buckling load, i.e. $[0.5, 1.9]$. The result is presented in Figure 5.2.

The horizontal deflection of the beam, $u(x)$, for particular values of parameters, given above, is plotted in Figure 5.3.

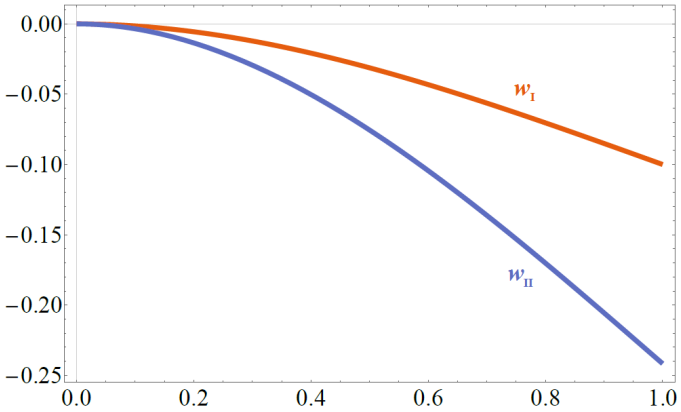

Figure 5.2: Transverse displacements within first- and second-order theories

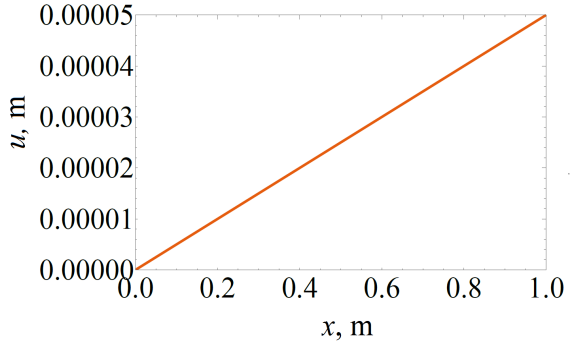

Figure 5.3: Deflection of the beam: First exemplary problem, first order theory

5.1.1.2 ROM solution

The model order reduction techniques described in Chapter 4 will now be applied. The FE model of this problem has 10 nodes and 30 DOFs. The results shown below are obtained for external loading localized on the 7th node. All input parameters are left the same as for the analytical solution, the precritical value of horizontal force $H = 1.9$ is considered to perform the MOR techniques. It is to be noted, that all computations below are done for 4 modes only: sensitivity analysis reveals, that independently from the order of the theory, when the number of modes increases, the approximation error decreases very rapipdly.

i) Krylov subspace method

The solution of the realisation of the force-location-parametrized problem with $\mu = 0.9$m taken as snapshot. Computations showed that the closer the snapshot under consideration is to the actual position of the loading, the more accurate are the results which should be expected. There are several techniques for a more sophisticated choice of snapshots used, for example, in the compact POD algorithms described in Chapter 4. These algorithms can be combined with any of the three techniques considered in this Chapter.

Figures 5.4–5.6 express the comparison of the FE approximate solution and that obtained using the Krylov subspace method based MOR within the first-, second- and third-order theories, respectively. Within the first-order theory, the two solutions are close to each other. Within the second-order theory, the two solutions differ slightly close to the $x = l$ end-point of the beam (see Figure 5.5). Figure 5.6 shows a significant mismatch between the two solutions. However, this mismatch can be reduced by increasing the number of modes.

It turns out, that for this problem 4 modes (see Figure 5.7) provide satisfactory results. Sensitivity analysis shows, that the error is a fast decreasing function of modes in the first-, second- and third-order theories (see Figure 5.8). It also follows

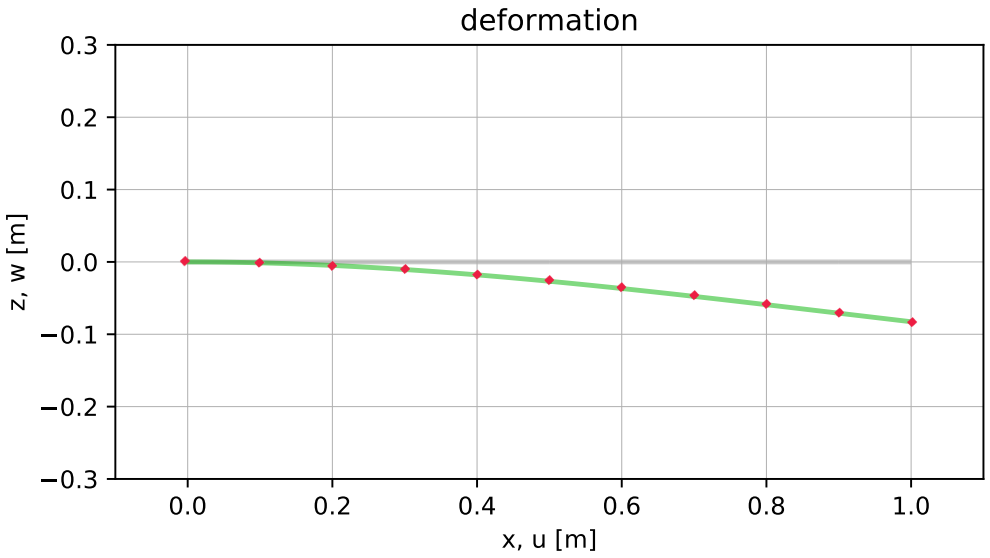

Figure 5.4: First exemplary problem: first order theory

from Figure 5.8, that within the first- and second-order theories the mismatch is almost the same for up to 20 modes and decreases significantly after 20 modes. Nevertheless, within the 3rd order theory the mismatch decreases significantly up to 10 modes and remains almost the same until 25 modes and then decreases again.

In Figure 5.8 the relative error sensitivity plots are introduced for Krylov subspace based MOR method within the first- and second-order theories, respectively. The upper plot shows, that the error between FEM and MOR solutions within the first order theory is about 3.2% for 4 modes and does not change dramatically for up to 20 modes. After that, the error starts to decrease and, for instance, for 30 modes it is about 0.1%. On the other hand, it is apparent from the lower plot, that for 4 modes the relative error for the second order theory is about 2.9%, which is almost the same for up to 25 modes, and then it decreases dramatically

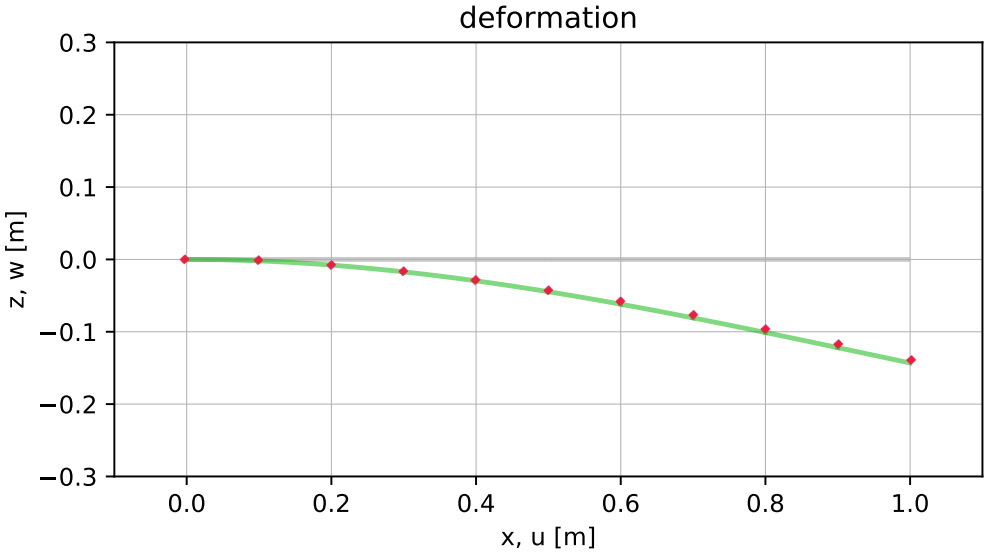

Figure 5.5: First exemplary problem: second order theory

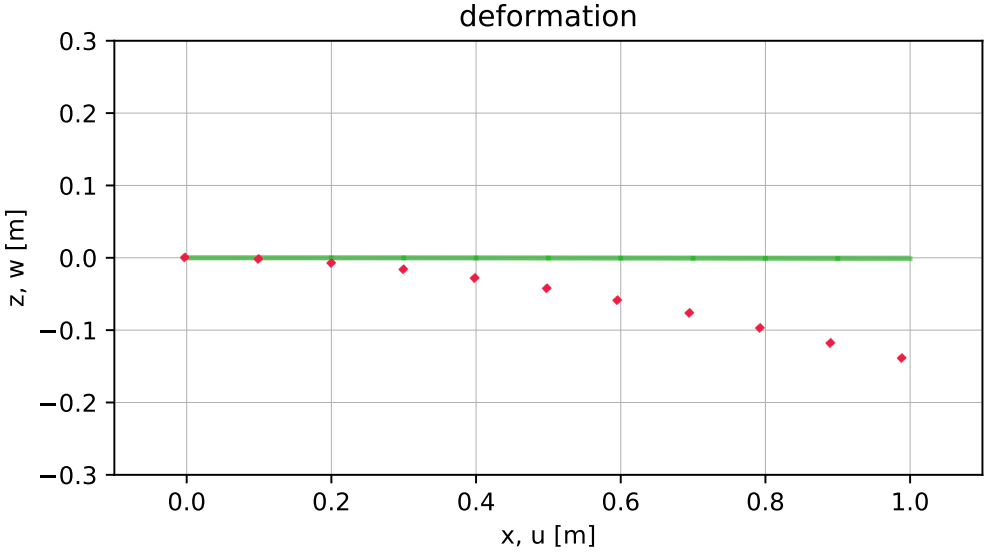

Figure 5.6: First exemplary problem: third order theory

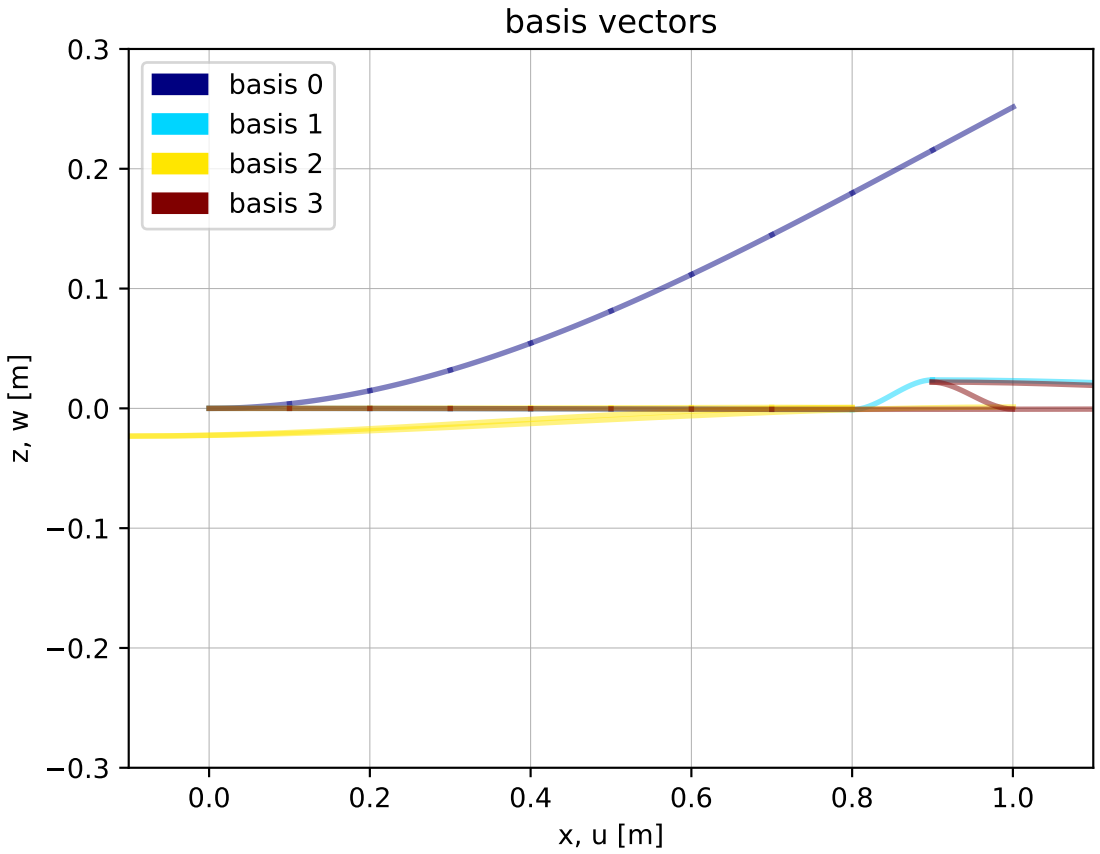

Figure 5.7: Basis of projection space for Krylov subspace method: first exemplary problem

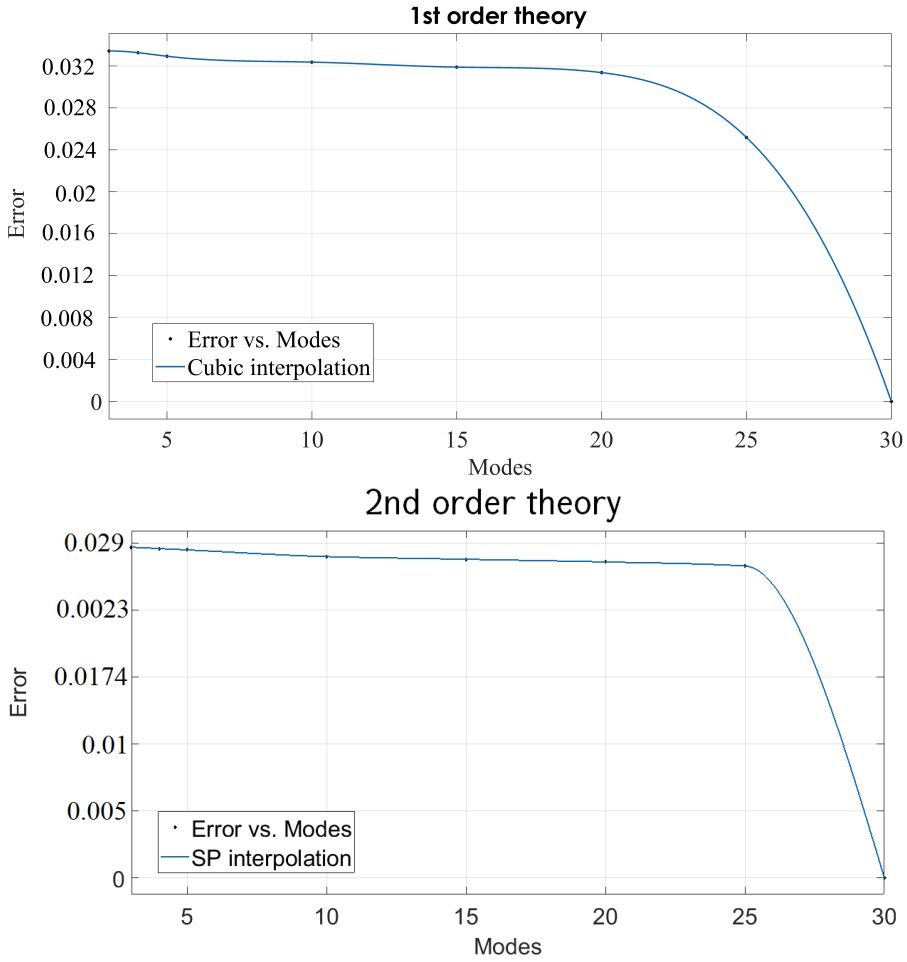

Figure 5.8: Error vs modes in Krylov subspace based MOR: first exemplary problem

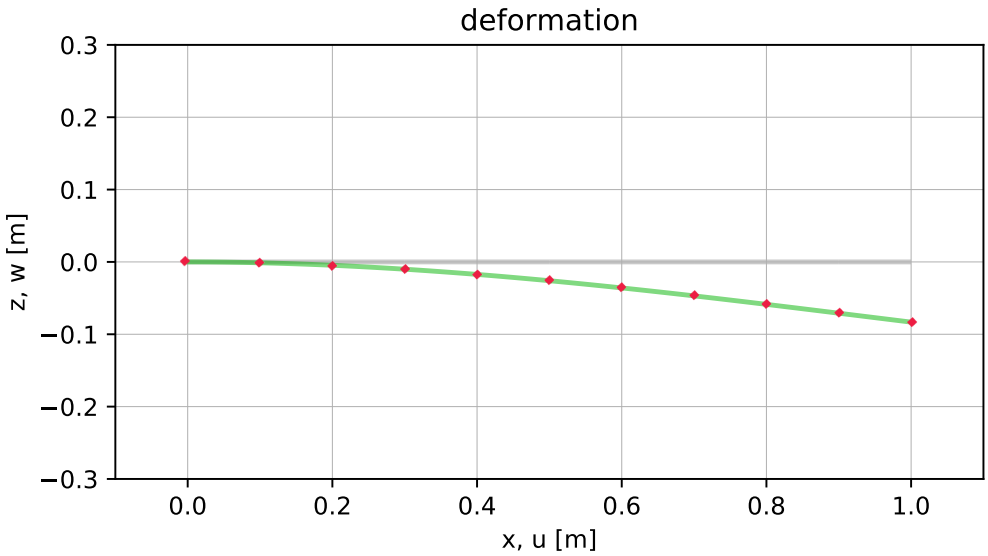

Figure 5.9: First exemplary problem: first order theory

ii) Inexact Krylov subspace method

The solution of the realisation of the force-location-parametrized problem with $\mu = 0.8$ m and $\mu = 0.9$ m taken as snapshots.

Figures 5.9–5.11 express the comparison of the FE solution and that obtained using the inexact Krylov subspace method based MOR within the first-, second- and third-order theories, respectively. The two solutions are sufficiently close within the first order theory. Within the second- and third-order theories the mismatch of the two solutions becomes significant when approaching the $x = l$ end of the beam.

The mismatch within the second- and third order theories can be reduced by increasing the number of modes. As above, once again only 4 modes are used here to perform the reduction (see 5.12). Sensitivity analysis reveals a rapid decrease in error with an increase in modes (see Figure 5.13). Moreover, within the first- and second order theories, up to 20 modes produce the same error, meanwhile within the third-order theory, using between 10 and 20 modes produces the same accuracy.

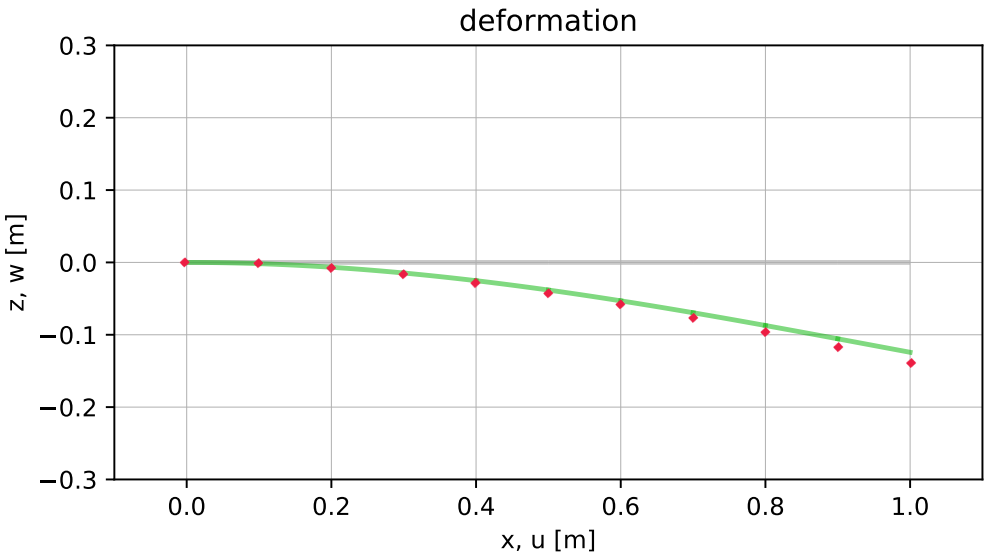

Figure 5.10: First exemplary problem: second order theory

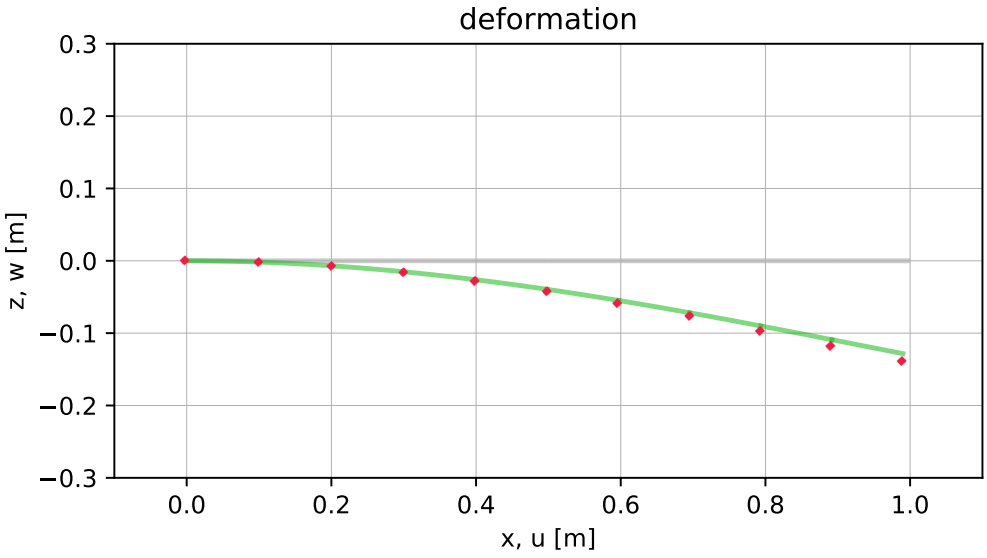

Figure 5.11: First exemplary problem: third order theory

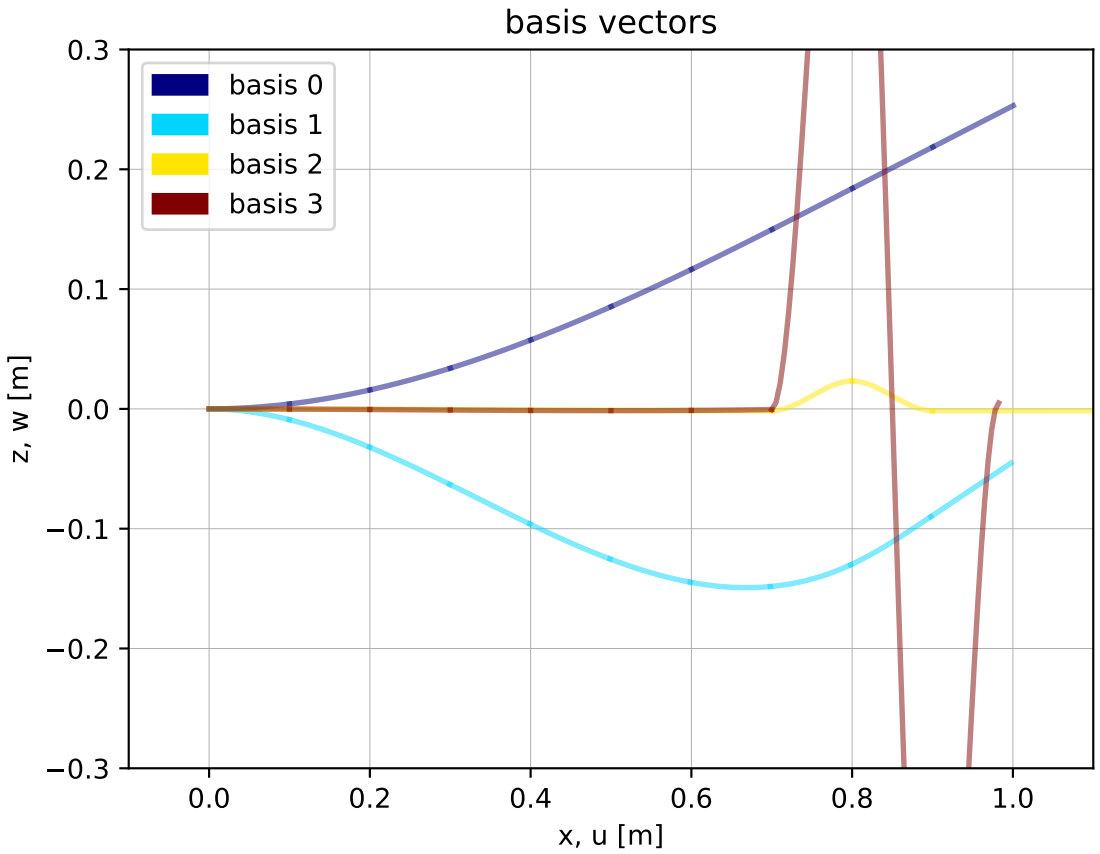

Figure 5.12: Basis of projection space for inexact Krylov subspace method: first exemplary problem

Figure 5.13 represents the relative error sensitivity plots for the inexact Krylov subspace based MOR method for the first-, second- and third-order theories, respectively. It is evident, that the error between the FEM and MOR solutions within the first- and second-order theories starts at 0.6% and 8%, respectively and then is almost the same for up to 20 modes, after which decreases dramatically. The relative error within the third order theory decreases from 8.2% (at the 4^{th} mode, which is used in the examples above), approaches 0.1% at 30 modes.

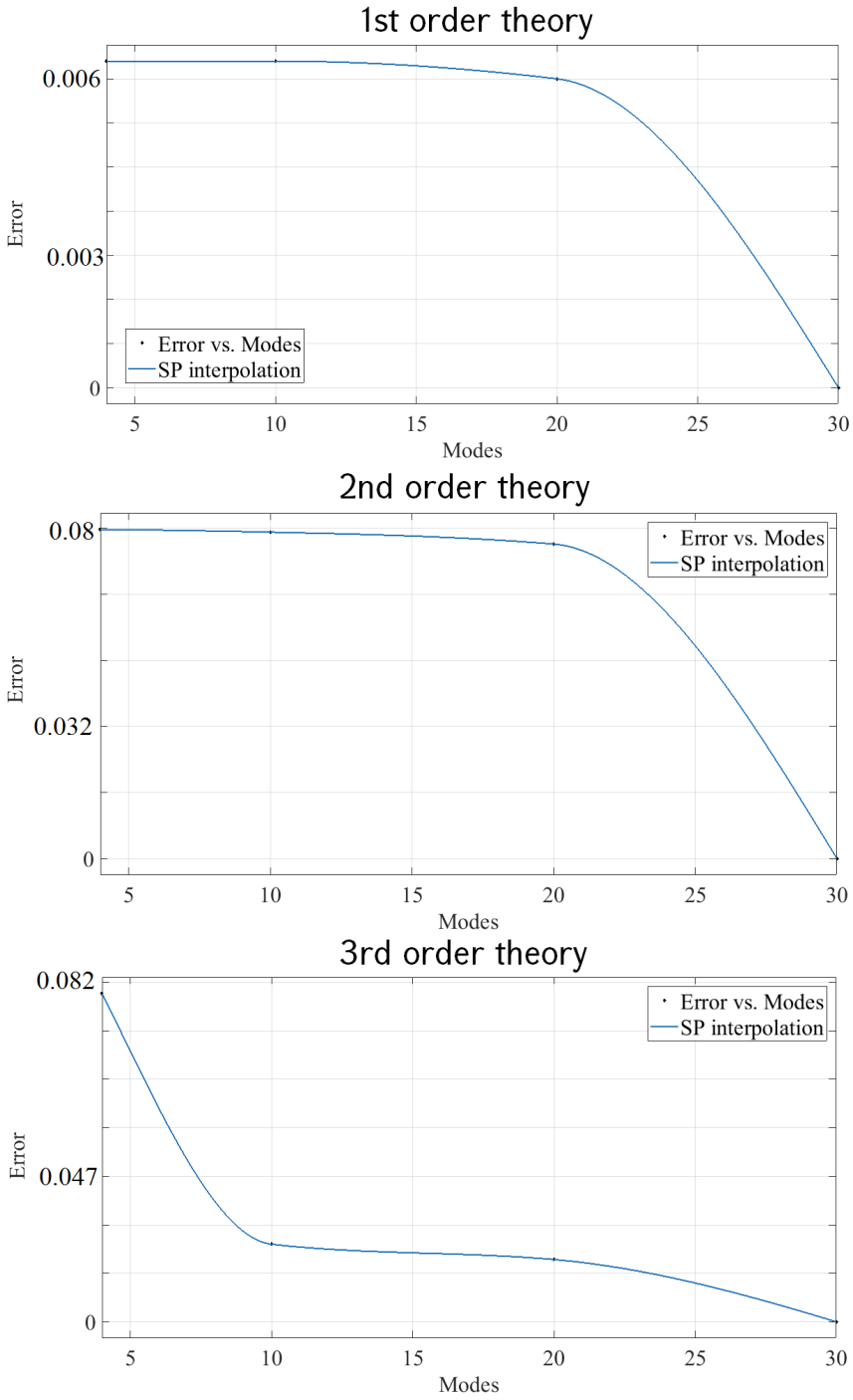

Figure 5.13: Error vs modes in inexact Krylov subspace based MOR: first exemplary problem

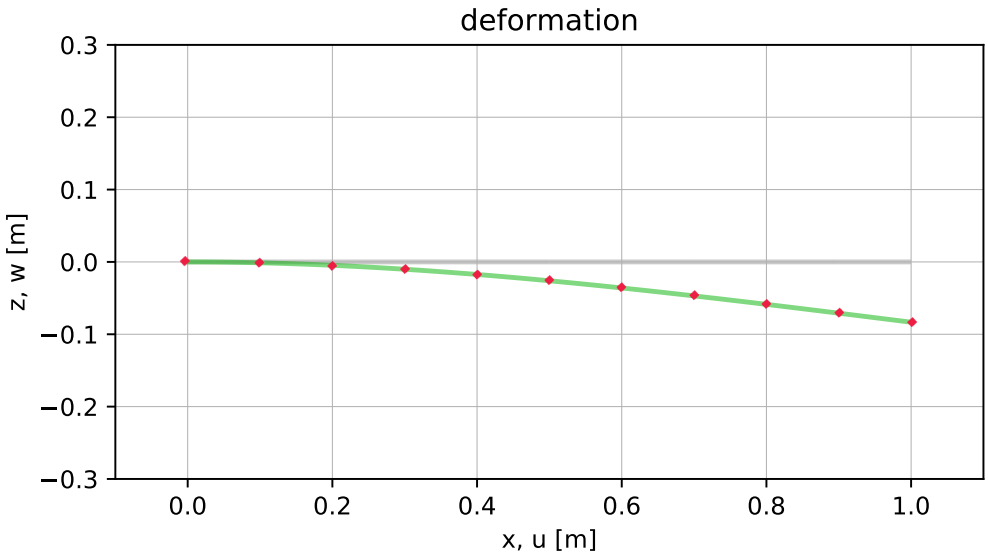

Figure 5.14: First exemplary problem: first order theory

iii) Snapshots based method

The solution of the realisation of the force-location-parametrized problem with $\mu = 0.6$ m, $\mu = 0.7$ m, $\mu = 0.8$ m and $\mu = 0.9$ m taken as snapshots.

Figures 5.14–5.16 express the comparison of the FE approximate solution and that obtained using snapshots based MOR within the first-, second- and third-order theories, respectively. This method provides a good approximation within all order theories.

It is to be noted, that also in this case only 4 modes are used (see Figure 5.17). Moreover, according to Figure 5.18 the error of approximation can be reduced by increasing the number of modes.

In Figure 5.18 relative error sensitivity is plotted for the full basis based MOR method for the first- and second-order theories, respectively. The error between the FEM and MOR solutions within the first-order theory starts at 0.1% (at the 4^{th}

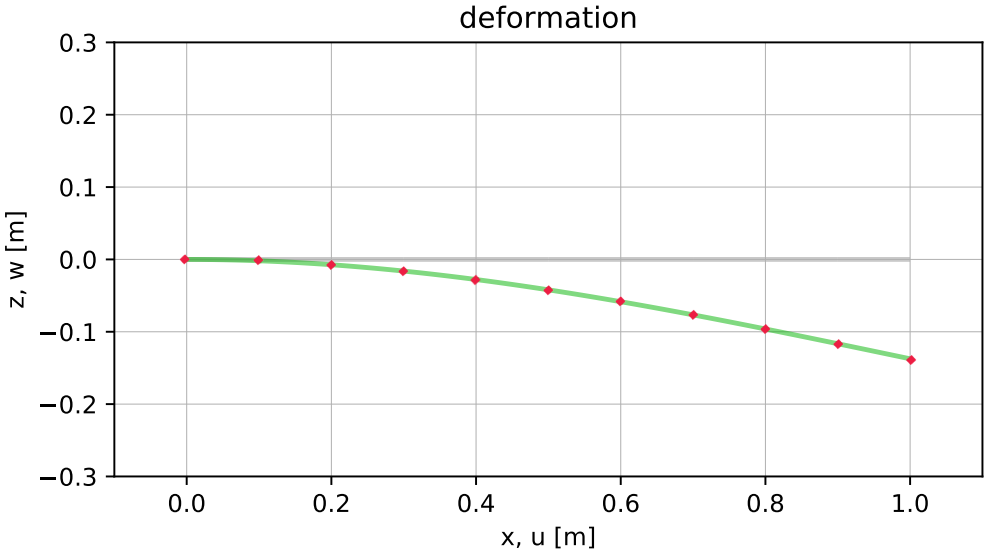

Figure 5.15: First exemplary problem: second order theory

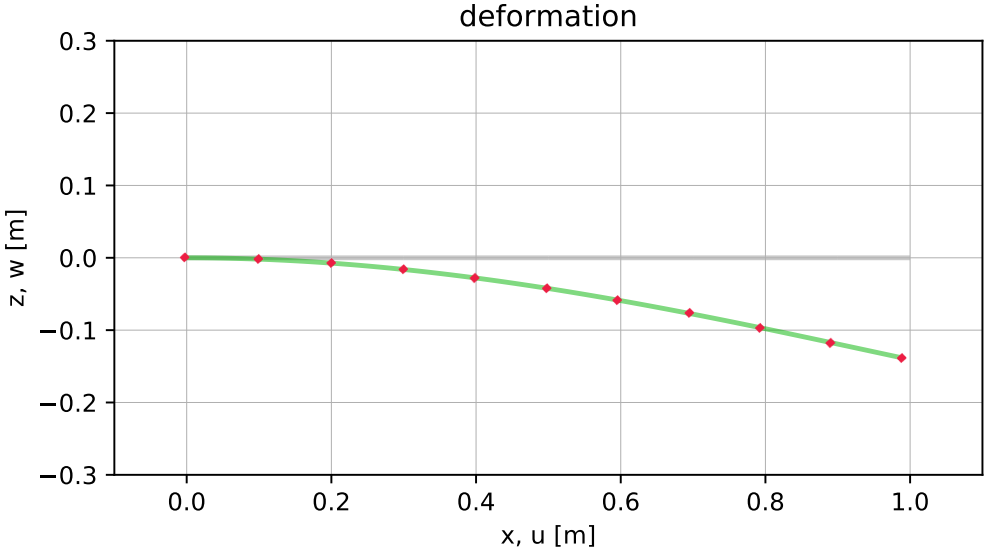

Figure 5.16: First exemplary problem: third order theory

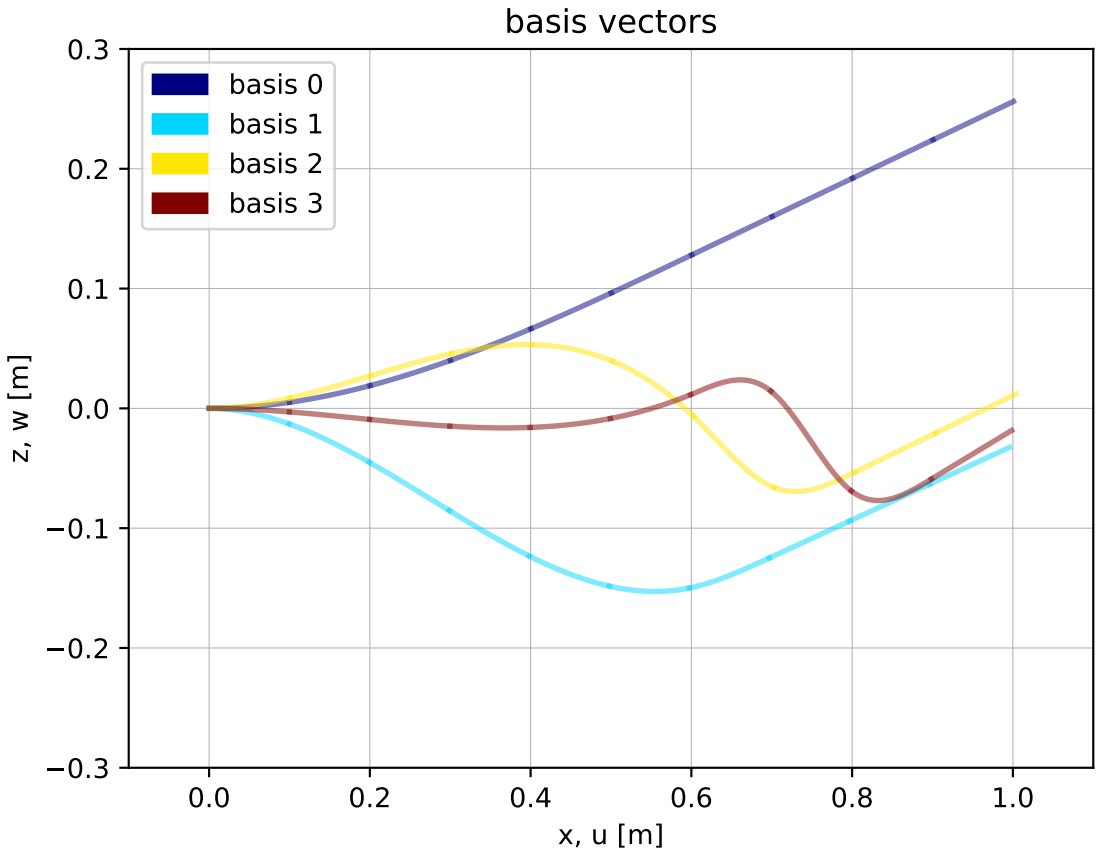

Figure 5.17: Basis of projection space for snapshots based method: first exemplary problem

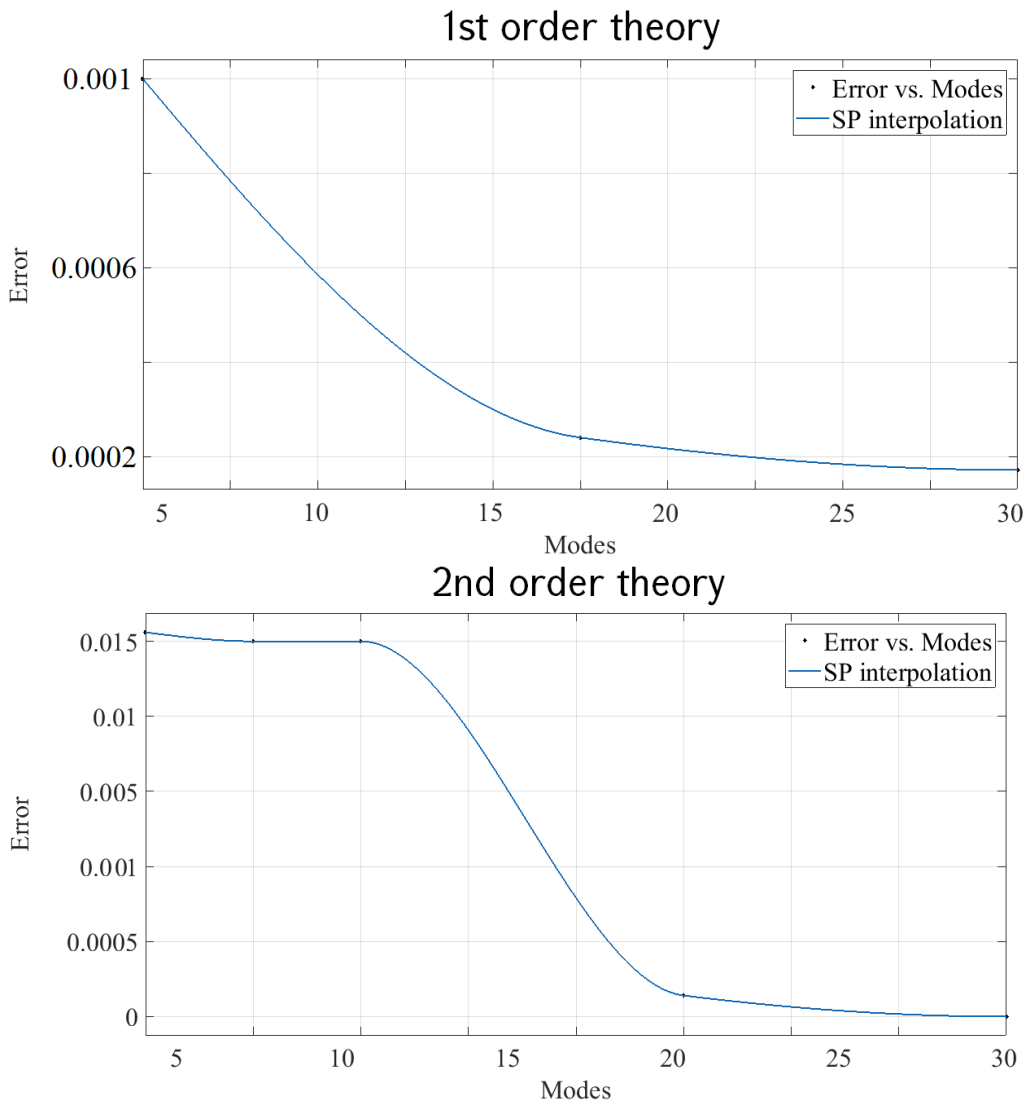

Figure 5.18: Error vs modes in snapshots based MOR: first exemplary problem

mode) and decreases very fast, approaching 0.02% at the 30^{th} mode. On the other hand, the error within the second order theory starts from 1.5% at the 4^{th} mode, remains almost the same up to the 10^{th} mode and then it decreases dramatically.

Theory	Krylov	Inexact Krylov	Snapshots
First order	0.031	0.0061	0.0011
Second order	0.0284	0.0808	0.0149
Third order	0.9914	0.0811	0.0084

Table 5.1: L^2 norm error estimates: first exemplary problem

In Table 5.1 L^2 norm error estimates are presented for all the aforementioned cases.

5.1.2 Second Exemplary Problem

Consider a horizontal beam of length l, clamped at $x = 0$ end, on the shiftable bearing at the other end and with an inner pin on distance l_1 from the clamped end. It is assumed, that longitudinal force H is applied at $x = l_1 + l_2 = l$, and that normal force P is applied at $x = l_1$ to the pin (see Figure 5.19).

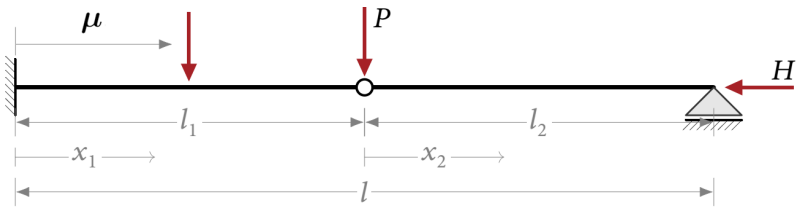

Figure 5.19: Compound Euler-Bernoulli beam: second exemplary problem

5.1.2.1 Exact solution

Input parameters are chosen to be $P = 0.1$ N, $H = 1$ N, $A = 10^{-4}$ m^2, $I_y = 10^{-9}$ m^4, $E = 2 \cdot 10^8$ N/m^2.

i) First order theory:

To solve the problem, we divide it into two domains: $0 \leq x_1 \leq l_1$ and $l_1 \leq x_2 \leq l_1 + l_2$. Both governing equations are of 4th order, 4 integration constants for each equation will be obtained. To determine them, 8 conditions are needed. The boundary conditions for the first part are

$$w_1(0) = 0,\ w_1'(0) = 0,\ w_1''(l_1) = 0,\ u_1(0) = 0, \tag{5.3}$$

and for the second part–

$$w_2''(l) = 0,\ w_2(l) = 0,\ u_2'(l) = -\frac{H}{EA}. \tag{5.4}$$

In order to derive continuous solution for all $0 \leq x \leq l$, compatibility conditions between w_1 and w_2 at $x = l_1$ must be satisfied:

$$\begin{gathered} w_1(l_1) = w_2(l_1),\quad w_1''(l_1) = w_2''(l_1),\quad EIw_1'''(l_1) = P + EIw_2'''(l_1), \\ u_1(l_1) = u_2(l_1). \end{gathered} \tag{5.5}$$

Therefore, the displacements are expressed as follows:

$$w_1(x_1) = -\frac{P}{EI}\frac{x_1^2\,(3l_1 - x_1)}{6},\quad 0 \leq x_1 \leq l_1, \tag{5.6}$$

$$w_2(x_2) = -\frac{P}{EI}\frac{l_1^3\,(l_2 - x_2)}{3(l_2 - l_1)},\quad l_1 \leq x_2 \leq l. \tag{5.7}$$

The deflection of the beam, $w(x)$, for particular values of parameters is plotted in Figure 5.20.

ii) Second order theory

The boundary and compatibility conditions read as

$$\begin{gathered} w_1(0) = 0,\quad w_1'(0) = 0,\quad w_1'''(l_1) = \frac{P}{EI} + \frac{H}{EI}w_1'(l_1),\quad w_1''(l_1) = 0, \\ w_1''(l_1) = w_2''(l_1),\quad w_2(l) = 0,\quad w_2''(l) = 0,\quad w_1(l_1) = w_2(l_1),\quad w_2''(l_1) = 0. \end{gathered} \tag{5.8}$$

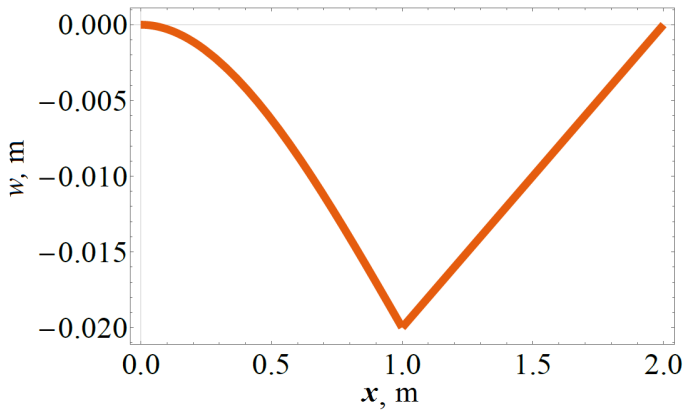

Figure 5.20: Deflection of the beam: second exemplary problem, first order theory

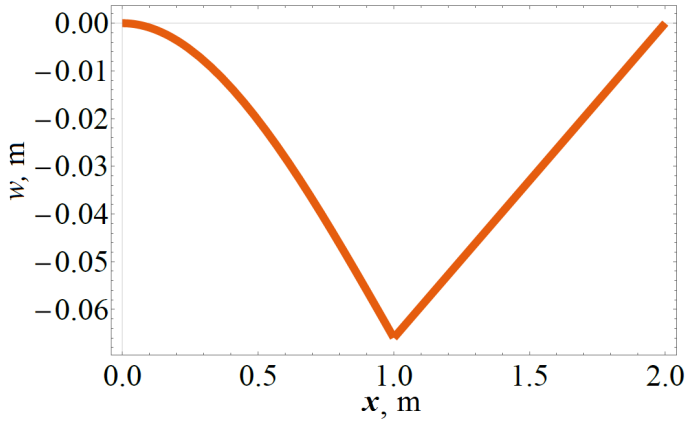

Figure 5.21: Deflection of the beam: second exemplary problem, second order theory

The displacements are determined as follows:

$$w_1(x_1) = \frac{P\left(kx_1\cos\left[kl_1\right] + \left(\sin\left[k\left(l_1 - x_1\right)\right] - \sin\left[kl_1\right]\right)\right)}{Hk\left(2 - \cos\left[kl_1\right]\right)}, \quad 0 \le x_1 \le l_1, \tag{5.9}$$

$$w_2(x_2) = \frac{P\left(l - x_2\right)\left(kl_1\cos\left[kl_1\right] - \sin\left[kl_1\right]\right)}{Hkl_2\left(1 - \cos\left[kl_1\right]\right)}, \quad l_1 \le x_2 \le l. \tag{5.10}$$

The deflection of the beam, $w(x)$, for particular values of parameters is plotted in Figure 5.21.

For the values of input parameters the critical H is computed to be $H \approx 1.0093$.

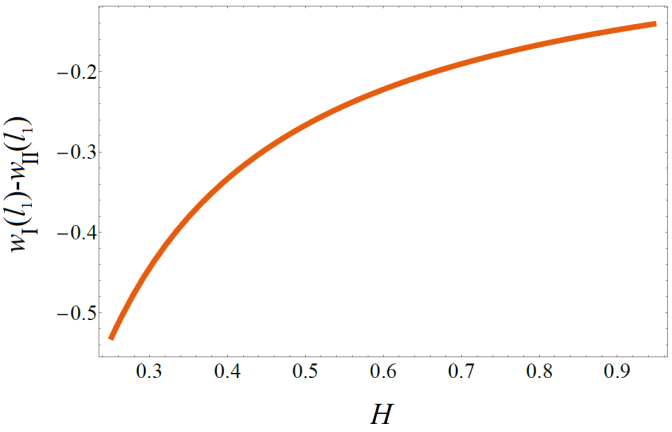

Figure 5.22: Difference between normal displacements within first and second order theories: Second example

In order to identify the difference between the first- and second-order theories, the transverse displacement, $w(x)$, from (5.6) and (5.10) is plotted at $x = l_1$ for H in the range $[0.25, 0.95]$. The result is presented in Figure 5.22.

5.1.2.2 ROM solution

The model order reduction techniques described in Chapter 4 are carried out on this exemplary problem. The FE model of this problem has 19 nodes and 57 DOF's. The results shown below are obtained for external loading localized on the 7th node. For the first- and second-order theories the value of the precritical horizontal force used is $H = 1$ N to perform the MOR techniques, while for the third order theory $H = 0.4$ is taken to run no more than 10 Newton-Raphson iterations.

i) Krylov subspace method

The solution of the realisation of the force-location-parametrized problem with $\mu = 0.9$ m taken as a snapshot.

Figures 5.23–5.25 express the comparison of the FE approximate solution and that obtained using Krylov subspace method based MOR within the first-, second-

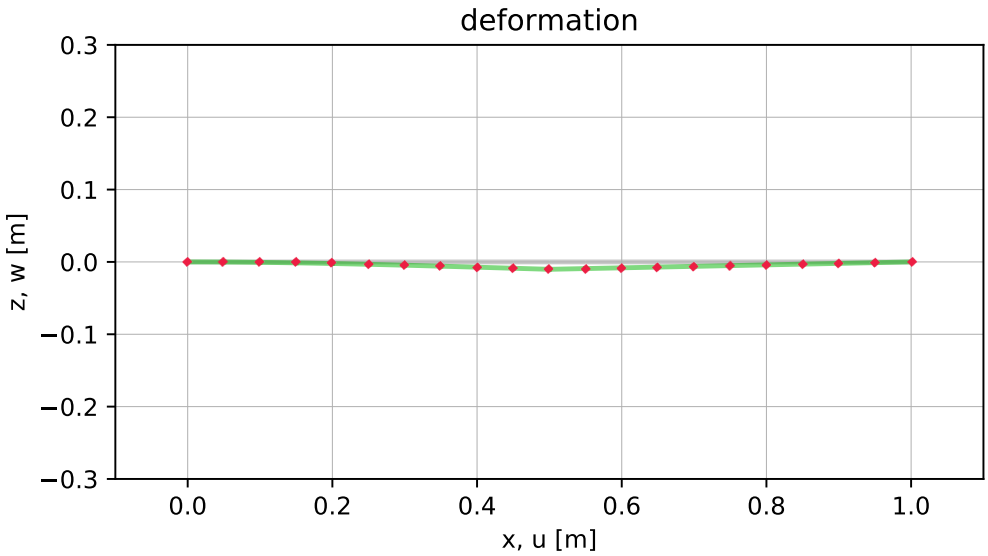

Figure 5.23: Second exemplary problem: first order theory

and third-order theories, respectively. Within the first-order theory the method provides a good approximation, whereas within the second- and third-order theories, mismatch is detected near the hinge.

The mismatch can be reduced by increasing the number of modes, which is chosen to be 4 (see Figure 5.26). For corresponding estimates of error dependence on the modes number within the first-, second- and third-order theories see Figure 5.27.

In Figure 5.27 relative error sensitivity is plotted for the Krylov subspace based MOR method for the first-order theory. The error between FEM and MOR solutions first decreases from 1.9% up to the 20^{th} mode, it then remains approximately the same up to the 30^{th} mode and then it decreases again.

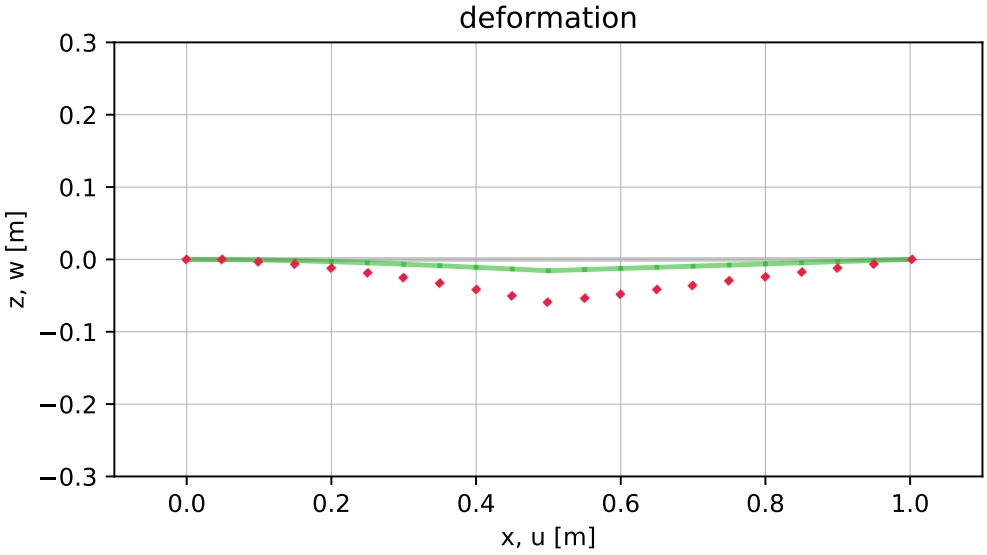

Figure 5.24: Second exemplary problem: second order theory

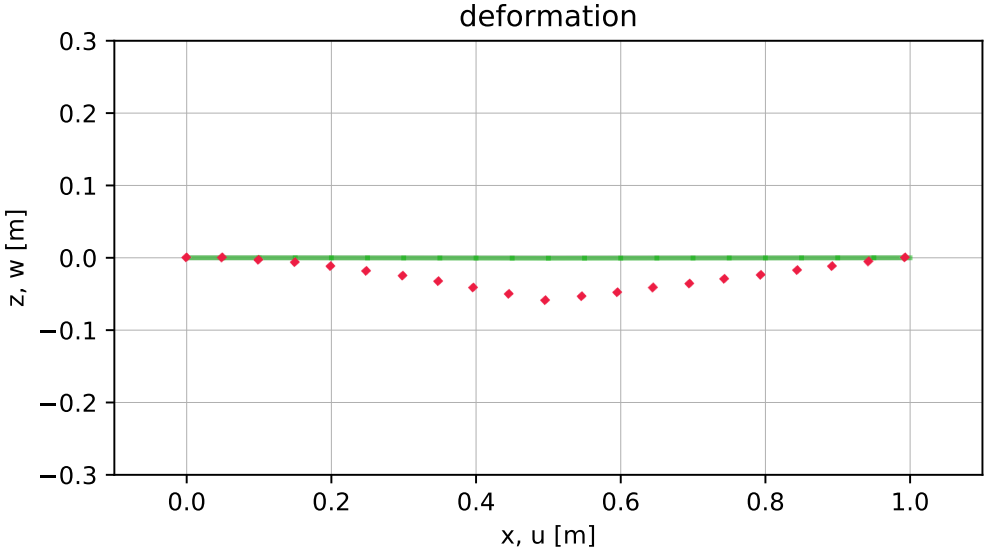

Figure 5.25: Second exemplary problem: third order theory

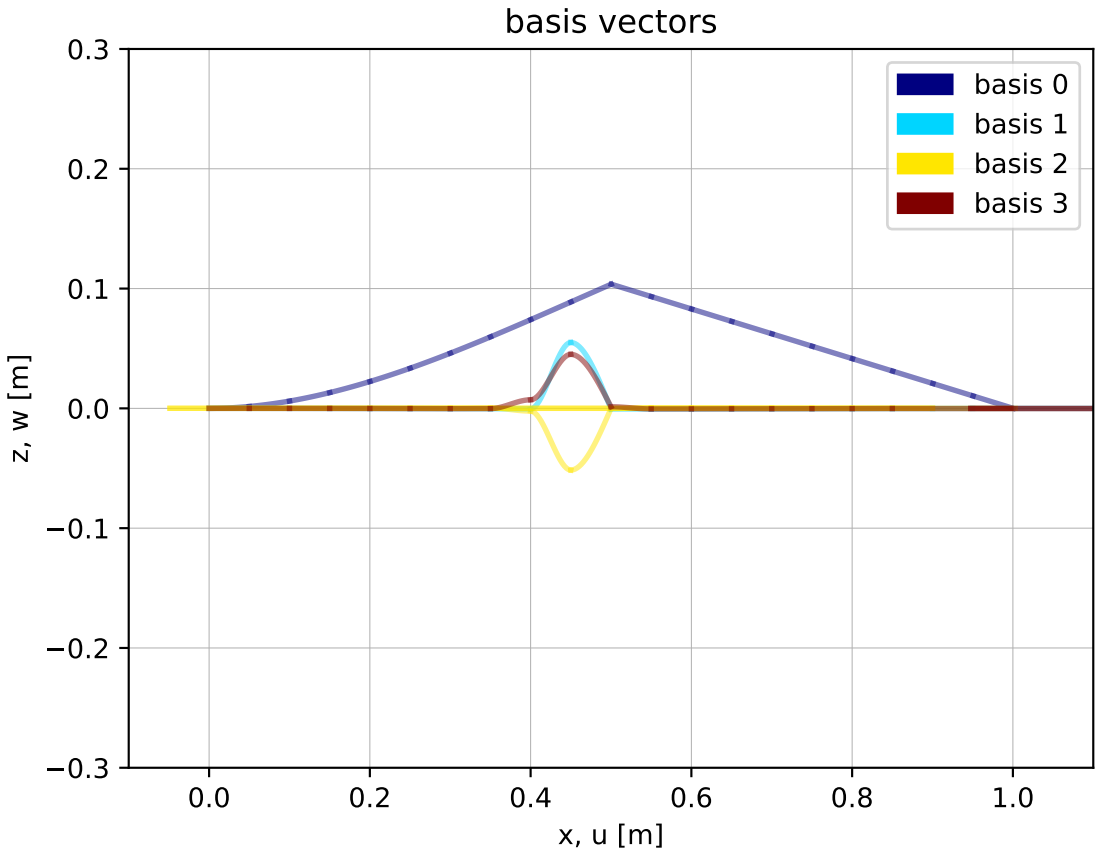

Figure 5.26: Basis of projection space for Krylov subspace method: second exemplary problem

Figure 5.27: Error vs modes in Krylov subspace based MOR: second exemplary problem

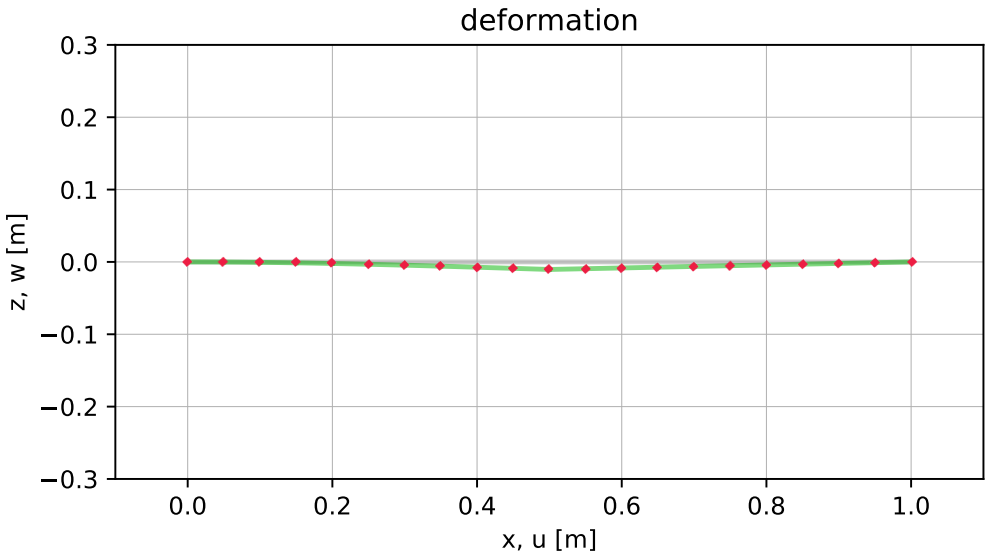

Figure 5.28: Second exemplary problem: first order theory

ii) Inexact Krylov subspace method

The solution of the realisation of the force-location-parametrized problem with $\mu = 0.8$ m and $\mu = 0.9$ m taken as snapshots.

Figures 5.28–5.30 express the comparison of the FE approximate solution and that obtained using the inexact Krylov subspace method based MOR. This method provides good approximation within the first- and third-order theories, while within the second-order theory a mismatch occurs near the hinge. It can be reduced by increasing the number of modes (4 are used here). The sensitivity analysis is introduced on Figure 5.32.

On Figure 5.31 the orthonormalized basis functions are plotted on which the projection subspace is spanned.

Figure 5.27 illustrates the relative error sensitivity on the number of modes for the inexact Krylov subspace based MOR method within the third-order theory. The

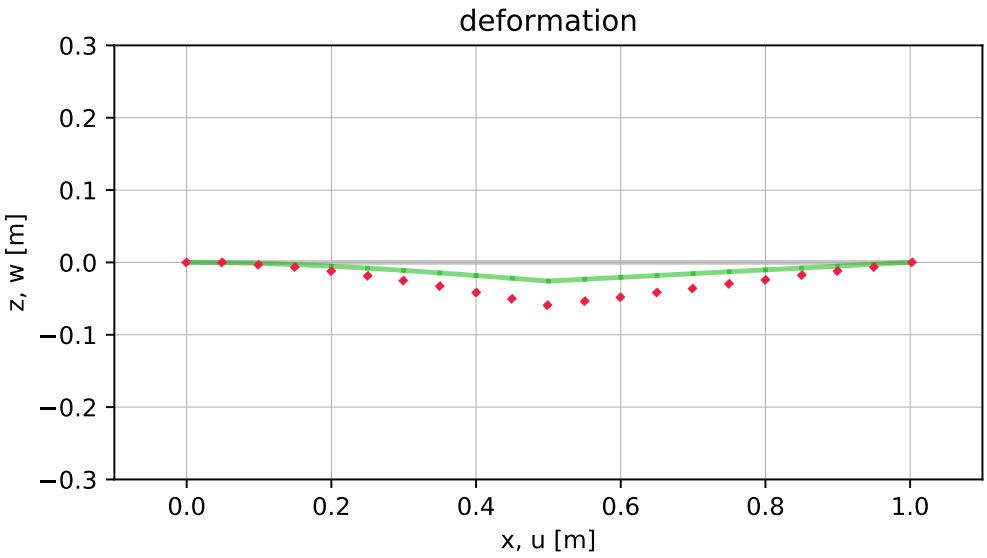

Figure 5.29: Second exemplary problem: second order theory

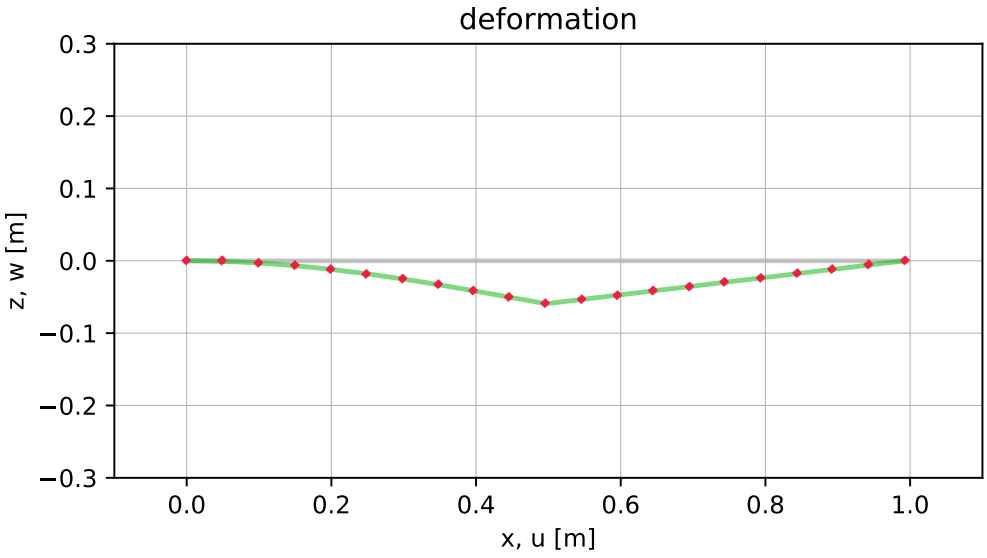

Figure 5.30: Second exemplary problem: third order theory

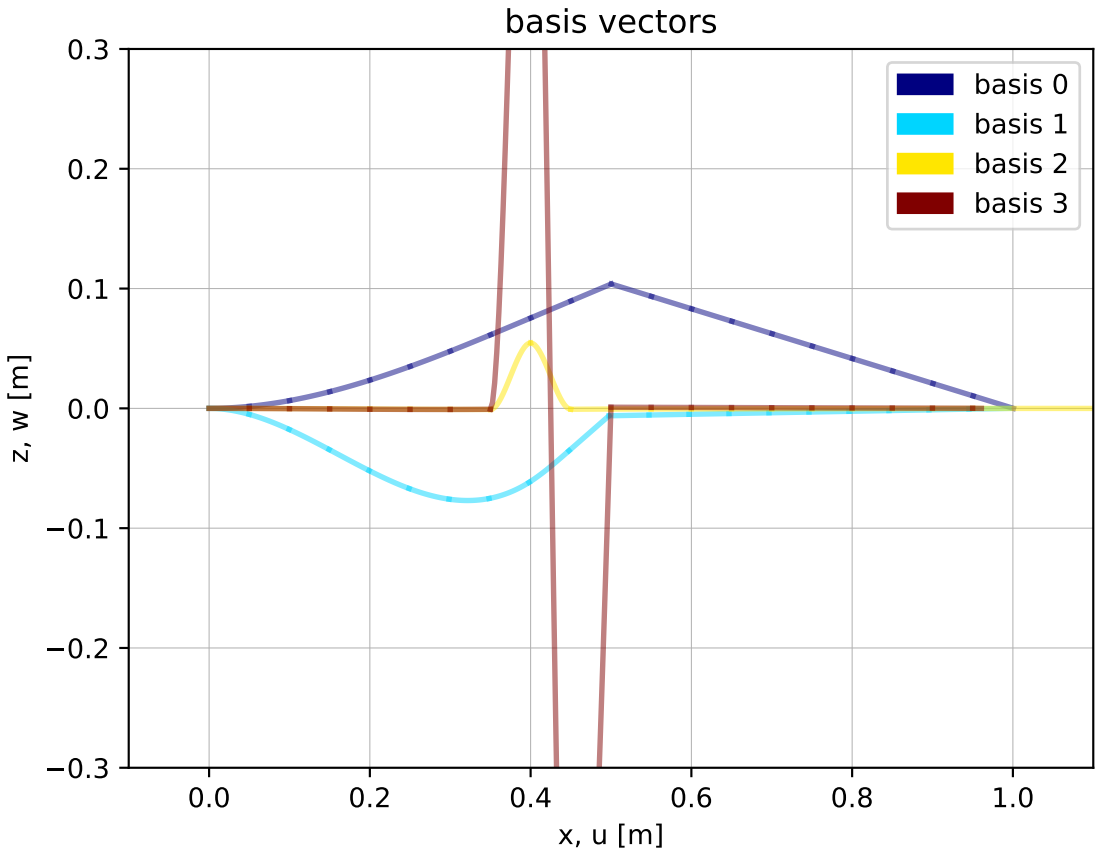

Figure 5.31: Basis of projection space for inexact Krylov subspace method: second exemplary problem

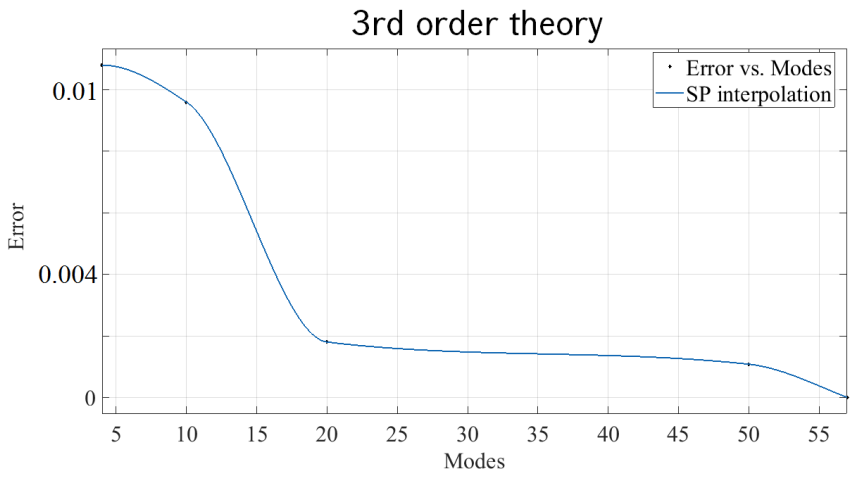

Figure 5.32: Error vs modes in inexact Krylov subspace based MOR: second exemplary problem

error between the FEM and MOR solutions decreases from 1.2% by about 5 times up to the 20^{th} mode, it then maintains almost the same value of 0.25% up to the 50^{th} mode and then it decreases dramatically.

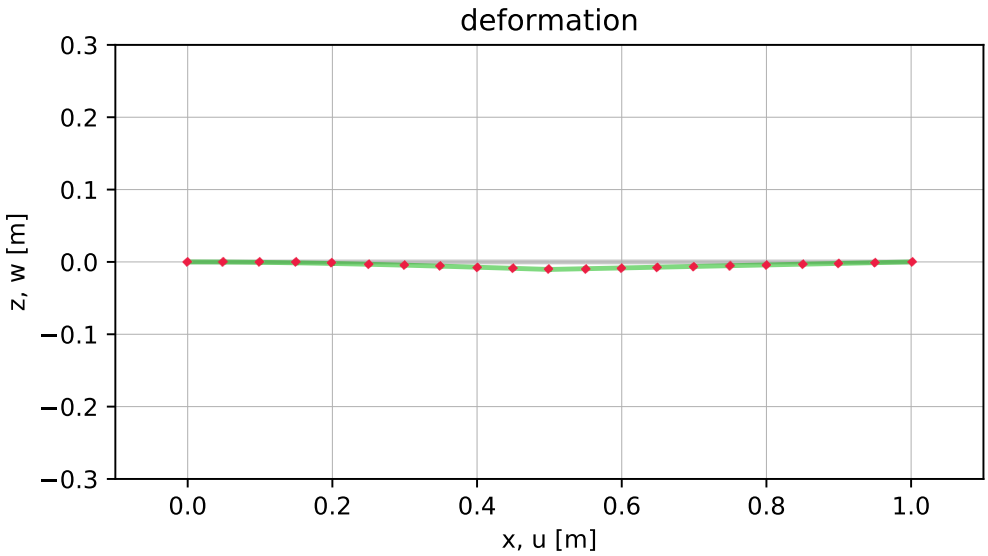

Figure 5.33: Second exemplary problem: first order theory

iii) Full basis based method

The solution of the realisation of the force-location-parametrized problem with $\mu = 0.6$ m, $\mu = 0.7$ m, $\mu = 0.8$ m and $\mu = 0.9$ m taken as snapshots.

Figures 5.33–5.35 express the comparison of the FE approximate solution and that obtained using snapshots based MOR within the first-, second- and third-order theories, respectively. Using only 4 modes, efficient approximation is obtained within the first- and third-order theories. A mismatch occurs between the two solutions, which is smaller than the corresponding mismatch with the previous method. The sensitivity analysis reveals very small approximation error. The corresponding modes are plotted on Figure 5.36.

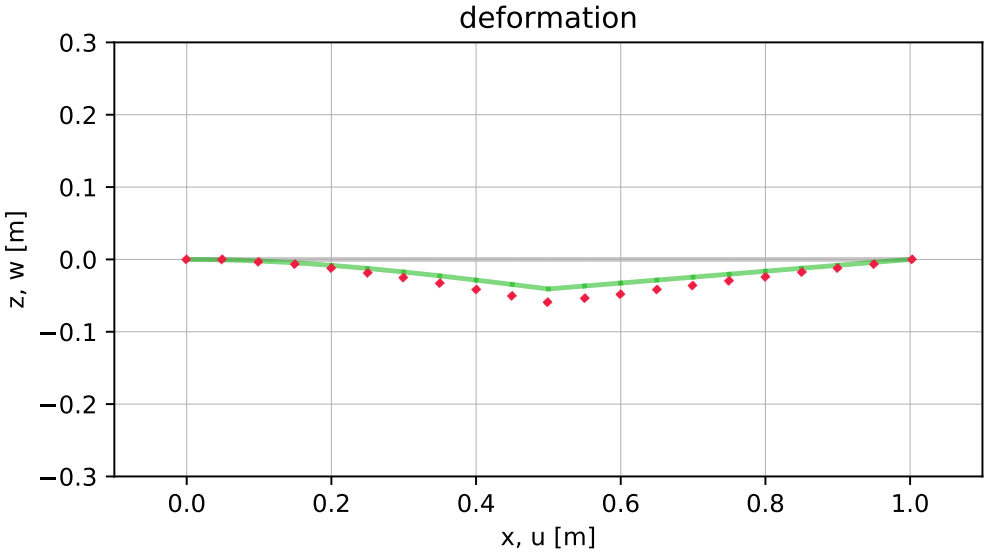

Figure 5.34: Second exemplary problem: second order theory

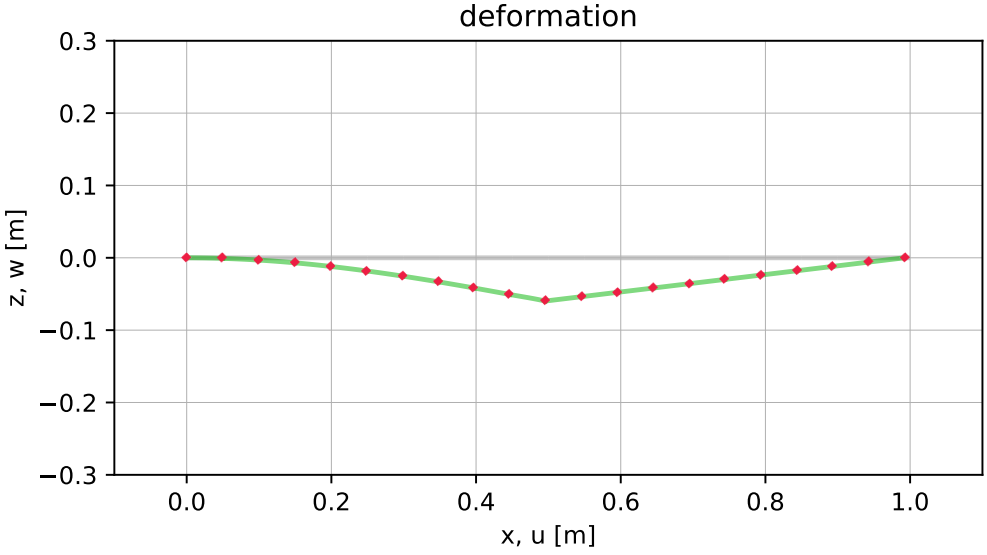

Figure 5.35: Second exemplary problem: third order theory

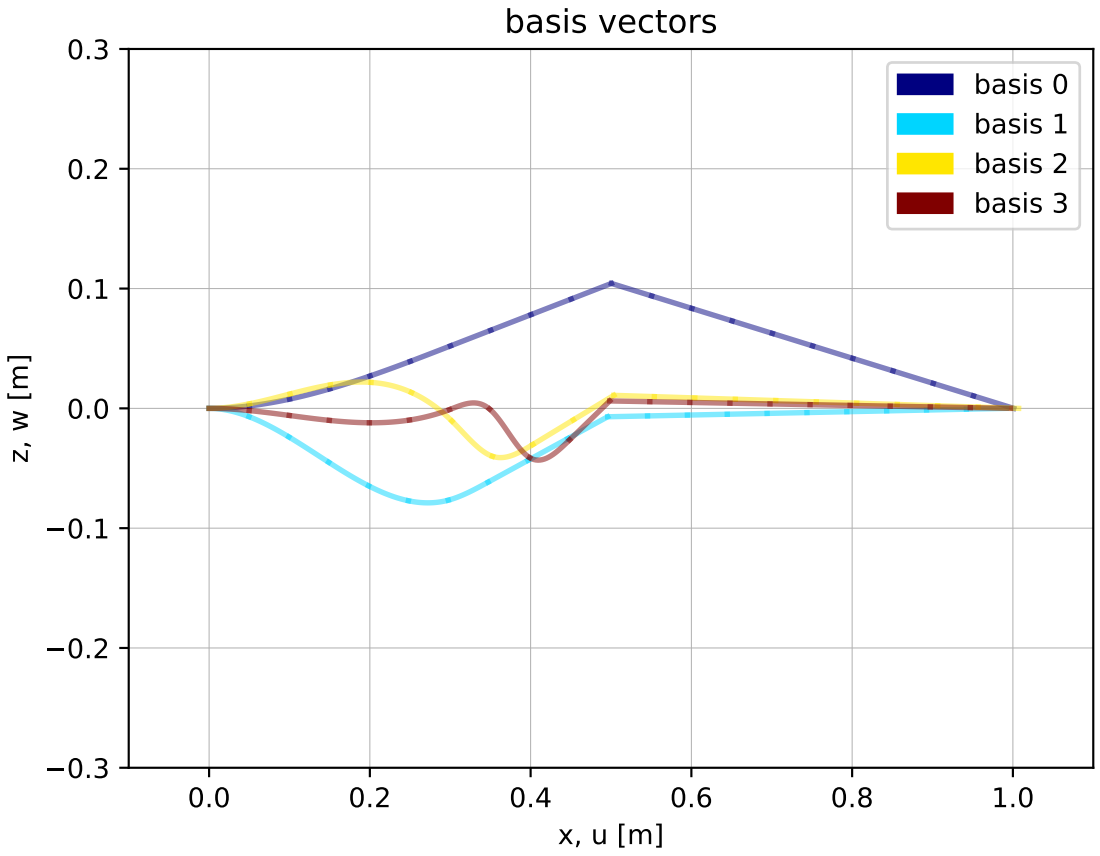

Figure 5.36: Basis of projection space for snapshot based method: second exemplary problem

Theory	Krylov	Inexact Krylov	Snapshots
First order	0.0267	0.0026	0.0011
Second order	0.7411	0.5733	0.3243
Third order	0.9905	0.0155	0.0103

Table 5.2: L^2 norm error estimates: second exemplary problem

In Table 5.2 L^2 norm error estimates are presented for all the aforementioned cases.

5.1.3 Third Exemplary Problem

In both of the problems above, the deflection $w(x)$ is almost the same within the second- and third-order theories. Nevertheless, it makes sense to consider them separately, especially when considering frame-shape structures. In analyzing such structures, the beams are separated from each other and the equilibrium of each one is considered separately. Eventually, the governing equations are coupled; the effect of the third order theory therefore becomes significant.

Consider a U-frame structure, loaded with a vertical and horizontal force in the middle (see Figure 5.37).

This example is considered only numerically, since its exact solution being straightforward, is lengthy. Input parameters are chosen $P = 0.1$ N, $H = 2$ N, $A = 10^{-4}$ m^2, $I_y = 10^{-9}$ m^4, $E = 2 \cdot 10^8$ N/m^2.

The model order reduction techniques described in Chapter 4 are performed on this exemplary problem. The FE model of this problem has 37 nodes and 111 DOF's. The results shown below are obtained for external loading localized on the 7th node.

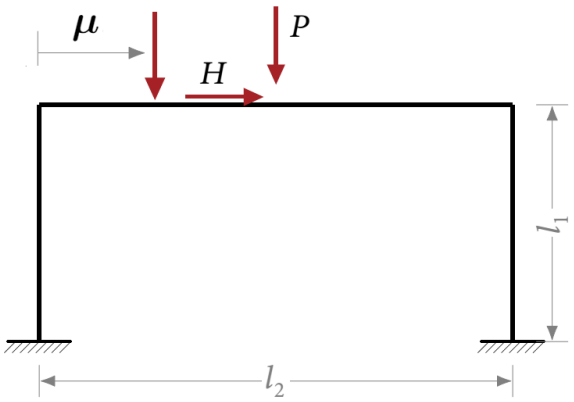

Figure 5.37: U-shape frame: Third exemplary problem

i) Krylov subspace method

The solution of the realisation of the force-location-parametrized problem with $\mu = 0.9$m taken as snapshot

Figures 5.38–5.40 express the comparison of the FEM solution and that obtained using the Krylov subspace method based MOR within the first-, second- and third-order theories, respectively. Restricting consideration to 4 modes only, approximation with a small relative error is derived within all three theories. The corresponding modes are plotted on Figure 5.41.

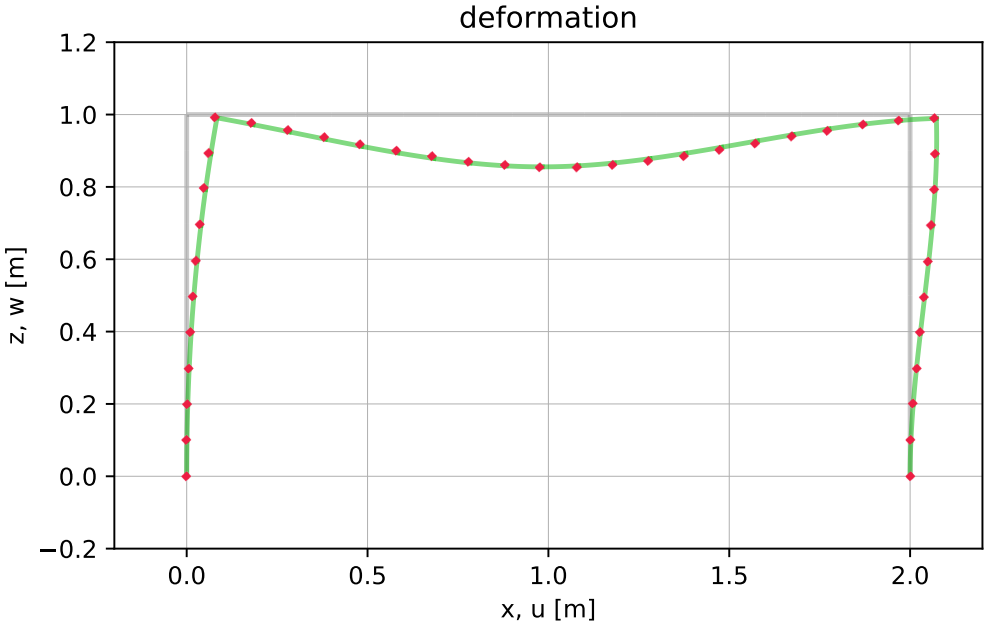

Figure 5.38: Third exemplary problem: first order theory

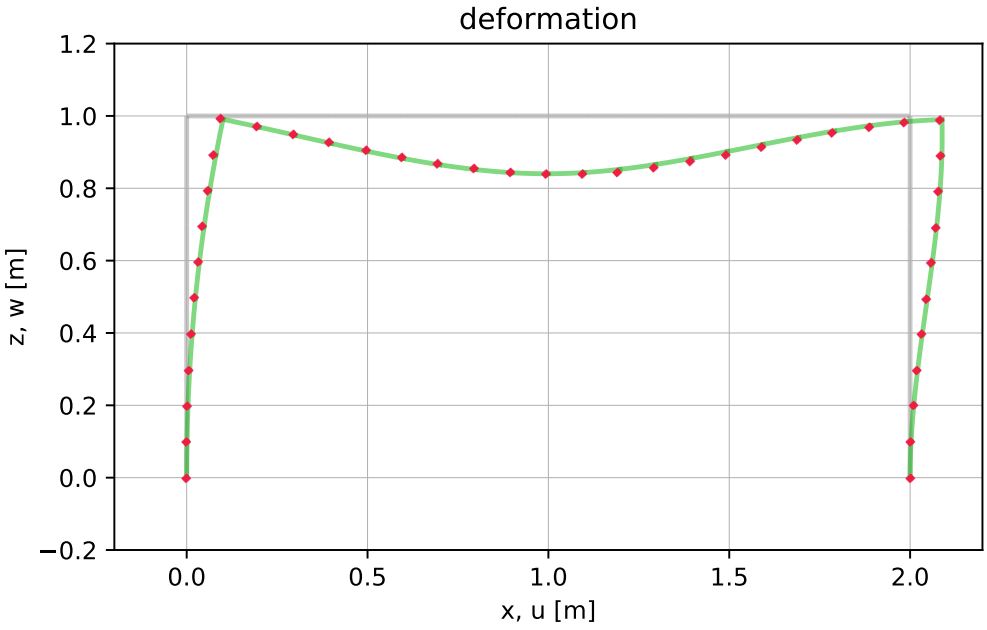

Figure 5.39: Third exemplary problem: second order theory

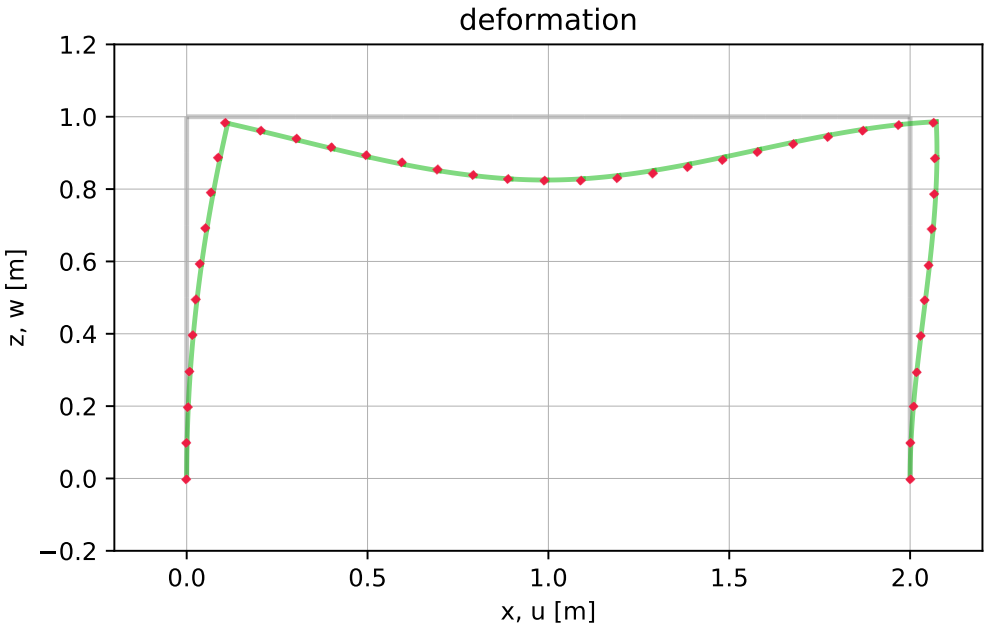

Figure 5.40: Third exemplary problem: third order theory

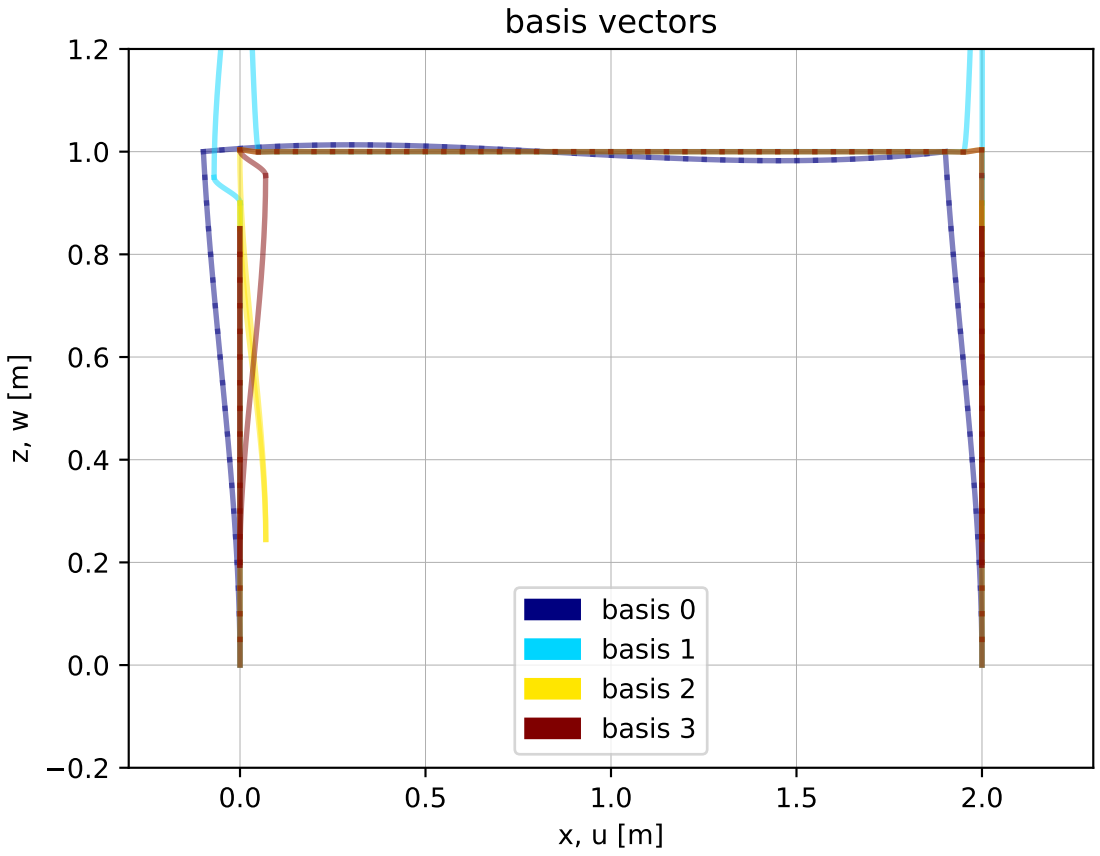

Figure 5.41: Basis of projection space for Krylov subspace based method: third exemplary problem

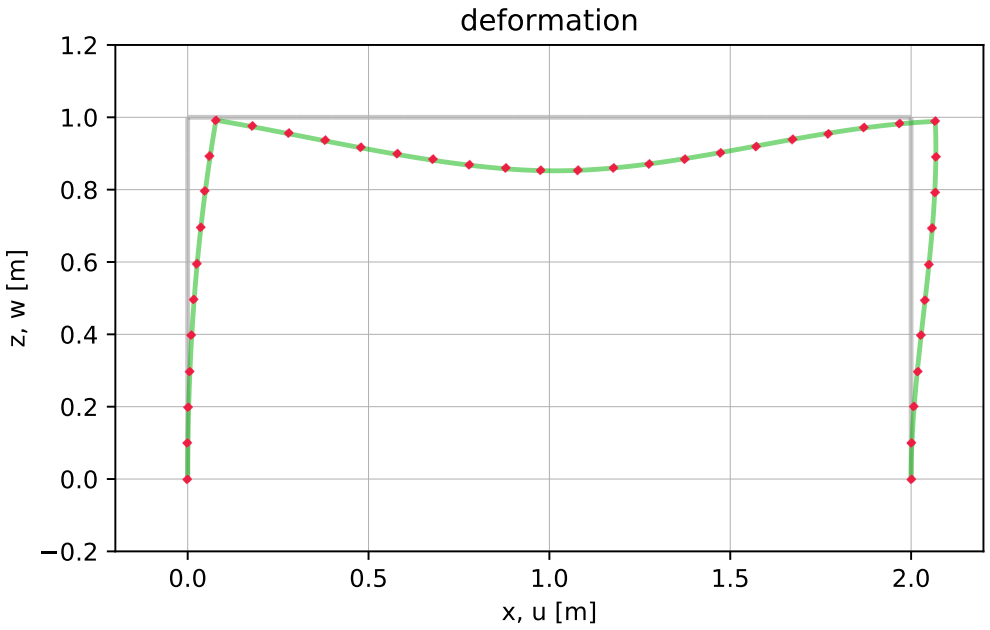

Figure 5.42: Third exemplary problem: first order theory

ii) Inexact Krylov subspace method

The solution of the realisation of the force-location-parametrized problem with $\mu = 0.8$ m and $\mu = 0.9$ m taken as snapshots.

Figures 5.42–5.44 express the comparison of the FE approximate solution and that obtained using the inexact Krylov subspace method based MOR within the first-, second- and third-order theories, respectively. Only 4 modes are considered, and approximation with a small relative error is derived within all three theories. The modes are plotted on Figure 5.45.

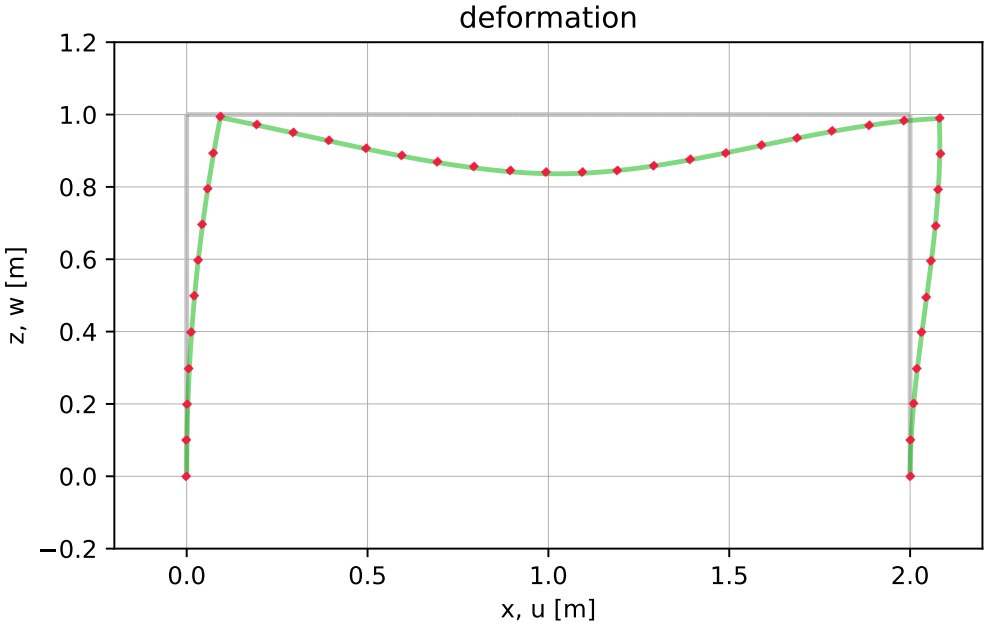

Figure 5.43: Third exemplary problem: second order theory

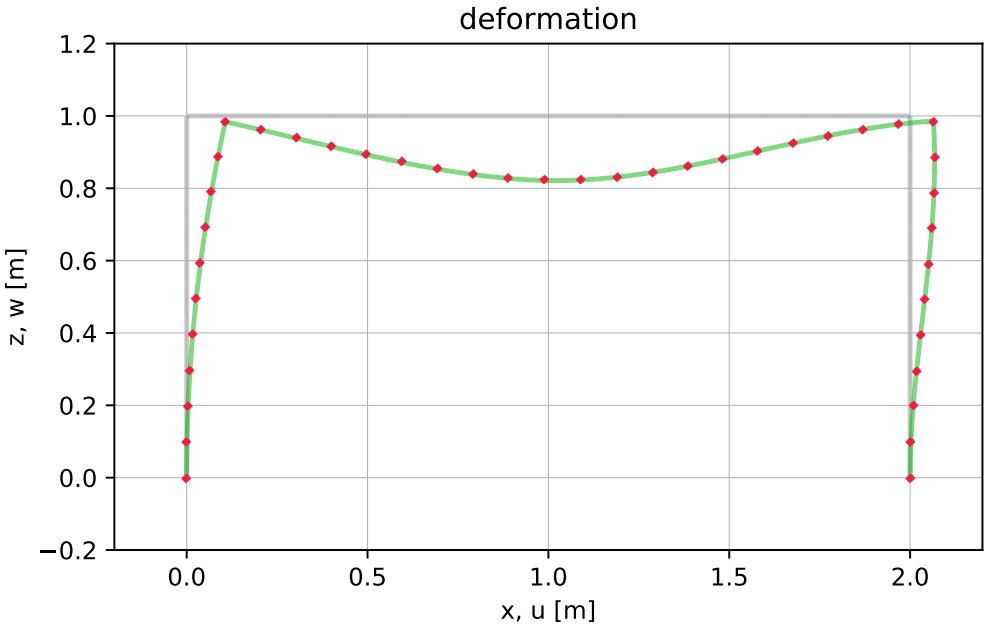

Figure 5.44: Third exemplary problem: third order theory

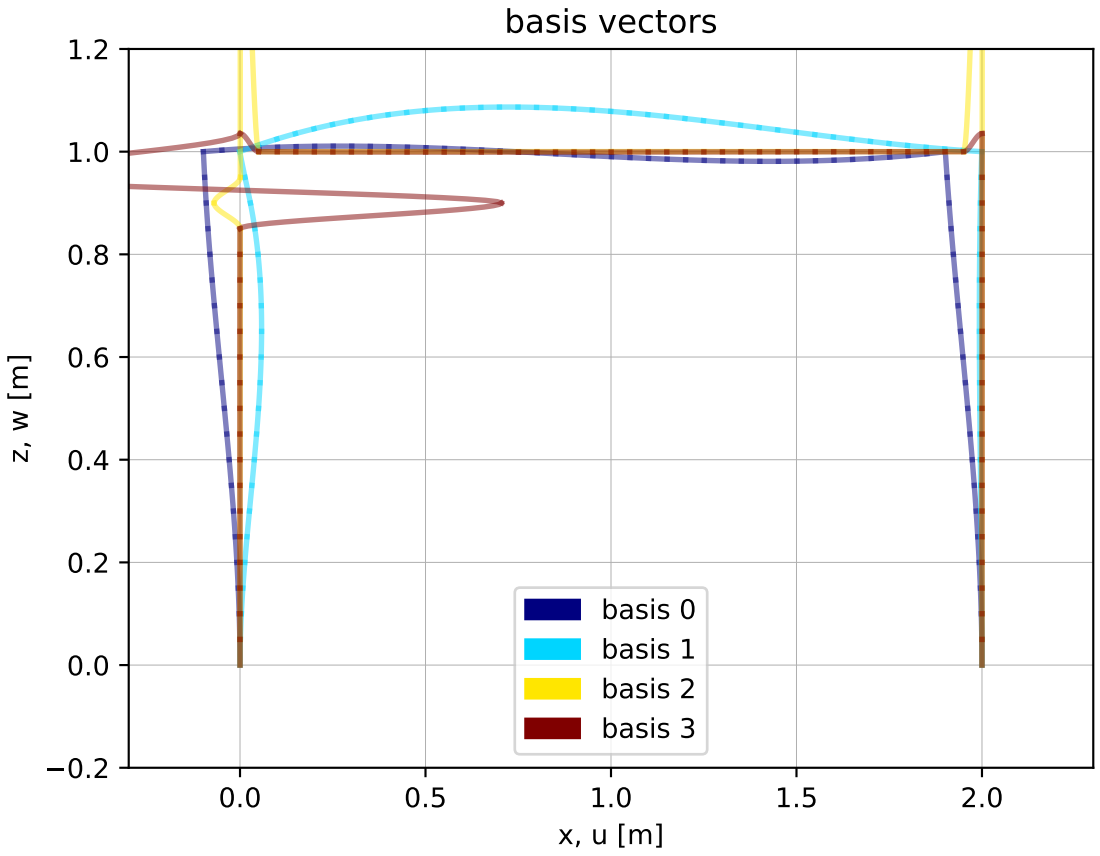

Figure 5.45: Basis of projection space for inexact Krylov subspace based method: third exemplary problem

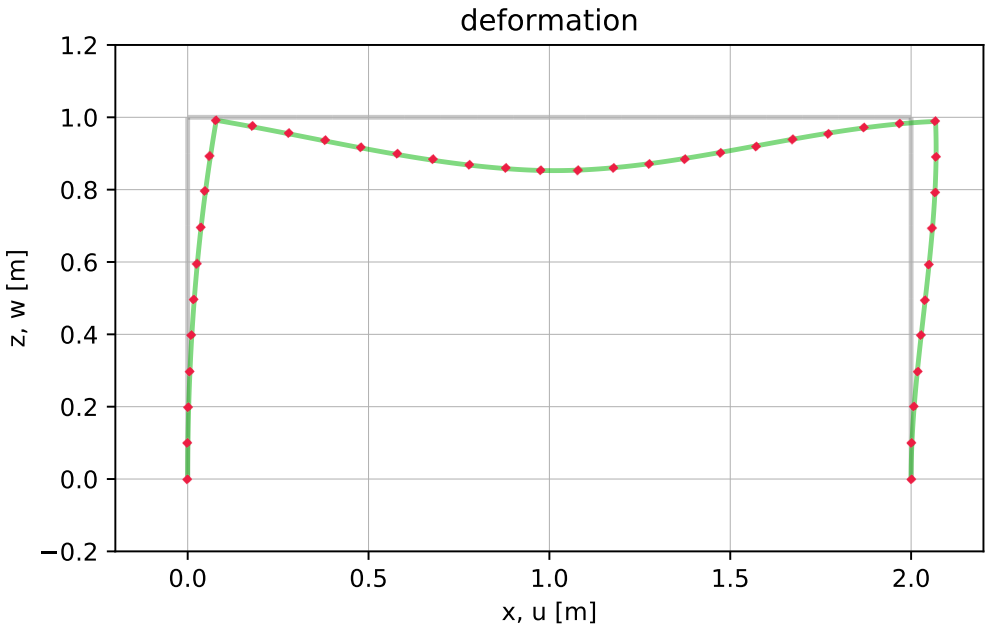

Figure 5.46: Third exemplary problem: first order theory

iii) Full basis based method

The solution of the realisation of the force-location-parametrized problem with $\mu = 0.6$ m, $\mu = 0.7$ m, $\mu = 0.8$ m and $\mu = 0.9$ m taken as snapshots.

Figures 5.46–5.48 express the comparison of the FE approximate solution and that obtained using snapshots based MOR within the first-, second- and third-order theories, respectively. Considering only 4 modes, approximation with a small relative error is derived within all three theories. See Figure 5.49 for corresponding modes.

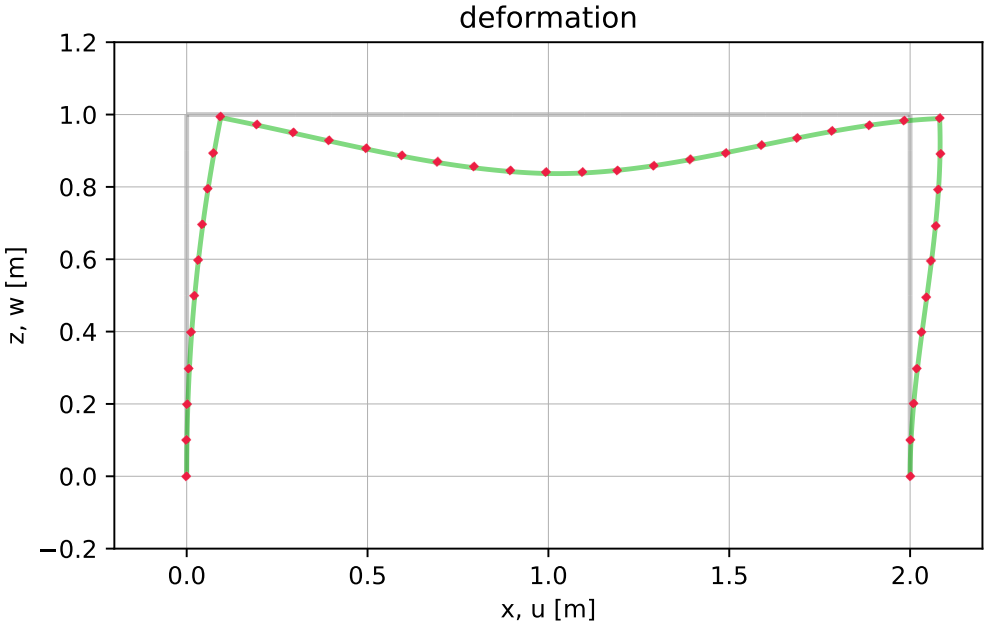

Figure 5.47: Third exemplary problem: second order theory

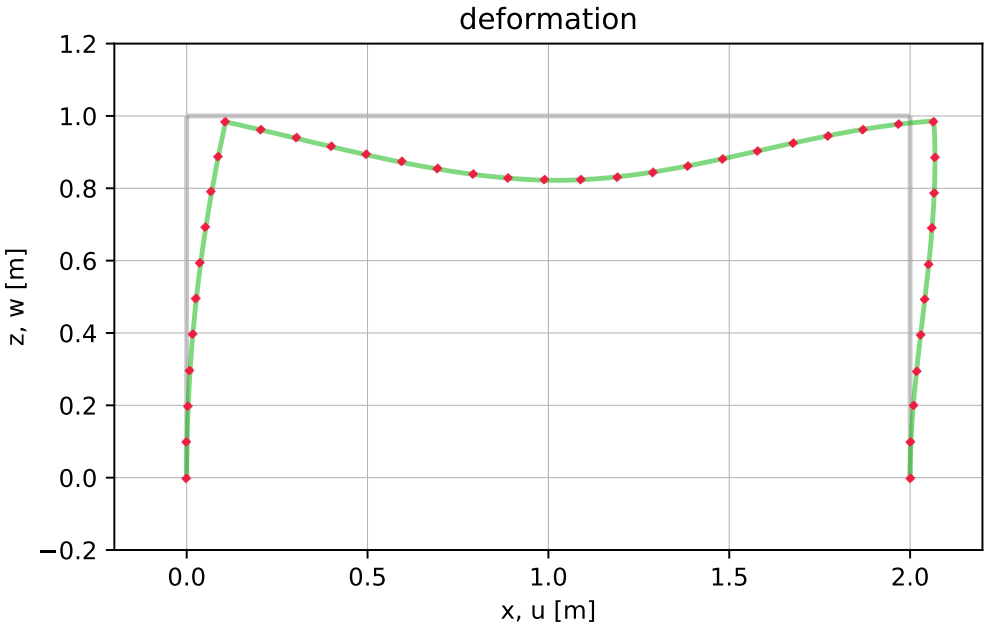

Figure 5.48: Third exemplary problem: third order theory

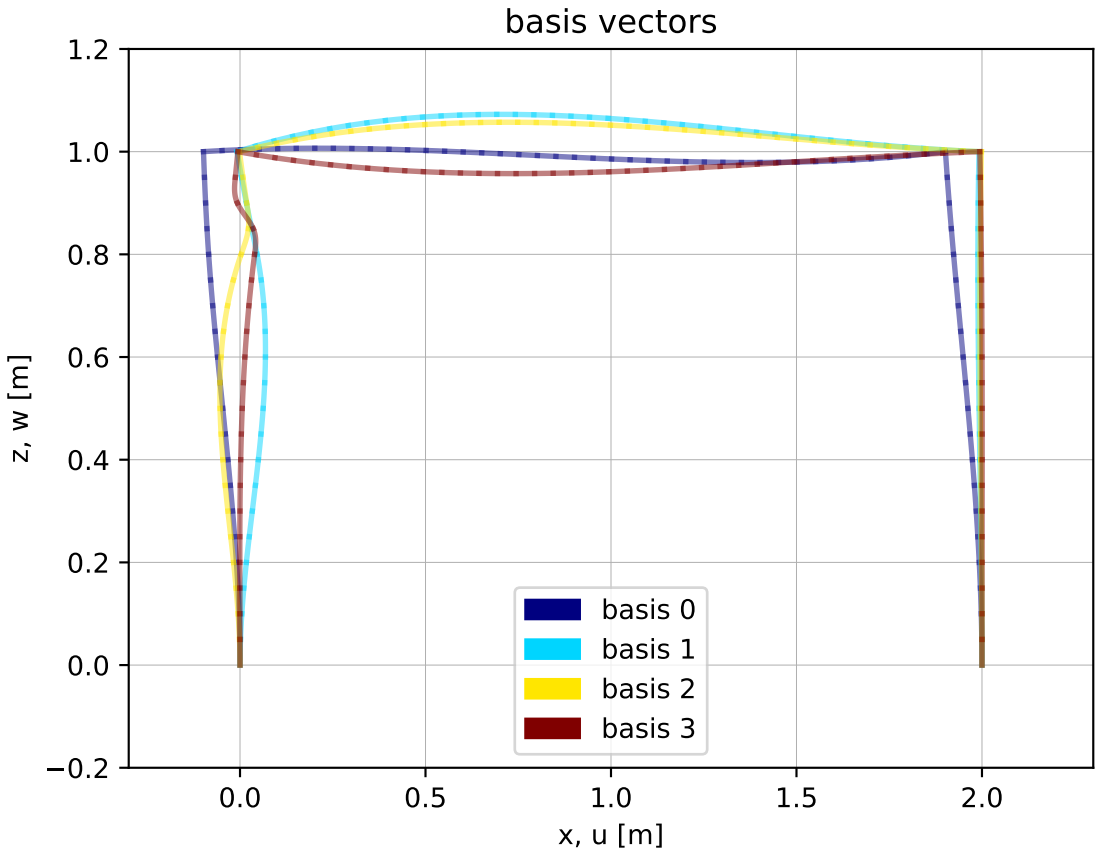

Figure 5.49: Basis of projection space for snapshots based method: third exemplary problem

Theory	Krylov	Inexact Krylov	Snapshots
First order	0.0729	0.0018	0.0018
Second order	0.0084	0.0019	0.0019
Third order	0.0084	0.0019	0.0018

Table 5.3: L^2 norm error estimates: Third exemplary problem

In Table 5.3 L^2 norm error estimates are presented for all the aforementioned cases.

Summary and Conclusions

This thesis is devoted to the comparison of model order reduction techniques to reduce the order of high-dimensional models which arise in non-linear static structural mechanics. The solution procedure to deal with a certain problem when a structure subjected to static loading is involved is usually the following. Using the finite element method, the governing structural equations are discretized and the corresponding system of algebraic equations is derived in terms of a tangent matrix. Usually, the dimension of the discretized system is fairly high. Therefore, the evaluation of the solution will be time-consuming. Model order reduction techniques make it possible to reduce the dimension of the discretized system and consequently to decrease computational costs.

Taking into account the features of static problems, modifications into an existing MOR method are carried out. Formally, the resulting methods are referred to as Krylov subspace, inexact Krylov subspace and full basis subspace-based MOR methods. The difference between these methods lies in the way the subspace is selected into which the discretized system has to be projected. In the case of the Krylov subspace-based MOR method, the set of orthonormal basis is achieved using the same snapshot, multiplied by increasing the powers of the tangent matrix. In the case of the inexact Krylov subspace-based MOR method, the set of orthonormal basis is enriched using increasing snapshots, multiplied by the tangent matrix. Finally, the full basis subspace-based MOR method uses increasing snapshots only (see Chapter 4).

The structures considered in this thesis are geometrically non-linear. This leads to a non-linear system of algebraic equations. The main contribution of this thesis is to build a MOR method to deal with non-linear systems. The main idea is to use Newton-Raphson iteration, which makes it possible to obtain a linear system at each iteration. Then any of the MOR methods described above can be used to reduce the order of the discretized linear system at each iteration.

Applications of this proposed MOR method are applied to particular non-linear systems:

i) a simple cantilever Euler-Bernoulli beam,

ii) two Euler-Bernoulli beams connected to each other by a joint,

iii) a frame structure.

Each problem is studied within the framework of three beam theories, formally mentioned as the first-, second- and third-order theories.

The problems are parametrized by the point of localization of the vertical loading. Then, computing the FE approximate solutions, snapshots for different values of the parameter are evaluated. In the final step, the computed snapshots are used to construct the corresponding projection subspaces in the Krylov subspace, inexact Krylov subspace and full basis subspace-based MOR methods. Observations showed that the closer the snapshot being considered is to the actual position of the loading, the more accurate are the results.

Each of the developed methods has its own advantages and disadvantages. Therefore, before applying one of them in order to analyse a particular structure, the following points must be taken into account.

- The disadvantage of the Krylov subspace-based MOR method is that it requires significant expenditure for the computation of the powers of the stiffness matrix. One of its advantages is that it uses only one snapshot to construct the projection subspace.

- The advantage of the inexact Krylov subspace-based MOR method (compared with the previous one) is that it is not necessary to compute any power of generally high-dimensional stiffness matrix. The disadvantage of this method is that more than 1 snapshot is required.

- The full basis subspace-based MOR method is computationally the most efficient method since it does not involve the stiffness matrix of the actual problem. However, it does require more snapshots than the previous two methods, which sometimes is impossible, for example, for the analysis of areas where sensors cannot be installed.

- In the sense of L^2-norm, the Krylov subspace-based method has the largest error, next comes the inexact Krylov subspace-based method and finally the full basis subspace-based method has the least error.

- Local effects (see the second exemplary problem) can also affect the accuracy of approximation with the Krylov and inexact Krylov subspace-based methods.

Bibliography

[1] Lucia D. J., Baren P. S., Silva W. A. Reduced-order modeling: new approaches for computational physics. *Progress in Aerospace Science*, 40(1-2):51–117, 2004.

[2] Noël A. T., Szabó B. A. Formulation of geometrically non-linear problems in the spatial reference frame. *International Journal for Numerical Methods in Engineering*, 40(8):1263–1280, 1997.

[3] Noor A. K., Balch C. D., Shibut M. A. Reduction methods for nonlinear steady-state thermal analysis. *International Journal for Numerical Methods in Engineering*, 20(7):1323–1348, 1984.

[4] Ryckelynck D., Chinesta F., Cueto E., Ammar A. On the a priori model reduction: Overview and recent bevelopments. *Archives of Computational Methods in Engineering*, 13(1):91–128, 2006.

[5] A. C. Antoulas, D. C. Sorensen, and S. Gugercin. *A survey of model reduction methods for large-scale systems*, 2001.

[6] Antoulas A. C. *Approximation of Large-Scale Dynamical Systems*. SIAM, Philadelphia, 2005.

[7] Carlberg K., Bou-Mosleh C., Farhat C. Efficient nonlinear model reduction via a least-squares Petrov-Galerkin projection and compressive tensor approxima-

tions. *International Journal for Numerical Methods in Engineering*, 86(2):155–181, 2013.

[8] Carlberg K., Farhat C. An adaptive pod-krylov reduced-order model for structural optimization. *8th World Congress on Structural and Multidisciplinary Optimization*, page 11 pages, 2009.

[9] Carlberg K., Farhat C. A low-cost, goal-oriented 'compact proper orthogonal decomposition' basis for model reduction of static systems. *International Journal for Numerical Methods in Engineering*, 86(3):381–402, 2011.

[10] Lanczos C. An iteration method for the solution of the eigenvalue problem of linear differential and integral operators. *Journal of Research of the National Bureau of Standards*, 45(4):225–280, 1950.

[11] Carlberg K., Farhat C., Cortial J., Amsallem D. The GNAT method for nonlinear model reduction: Affective implementation and application to computational fluid dynamics and turbulent flows. *Journal of Computational Physics*, 242:623–647, 2013.

[12] Davies J. M., Philip L., Heinz D. Second-order generalised beam theory. *Journal of Constructional Steel Research*, 31:221–241, 1994.

[13] Hermann A., Dinkler D. *Finite-Element-Methoden, Teil 2*. Springer, TU Braunschweig, Deutschland, 1990.

[14] Zienkiewicz O. C., Taylor R. L., Fox D. D. *The Finite Element Method for Solid and Structural Mechanics, 7th edn.* Elsevier, Oxford, 2014.

[15] de Villemagne C., Skelton R. E. Model reductions using a projection formulation. *International Journal of Control*, 46(6):2141–2169, 1987.

[16] Hahn J., Edgar T. F. An improved method for nonlinear model reduction using balancing of empirical grammians. *Computers & Chemical Engineering*, 26(10):1379–1397, 2002.

[17] Nayfeh A. H., Pai P. F. *Linear and Nonlinear Structural Mechanics*. John Wiley & Sons, New Jersey, 2004.

[18] Ciarlet Ph. G. *Mathematical Elasticity. Vol. I-III*. Elsevier, Amsterdam, 1994.

[19] Gilbert E. G. Functional expansions for the response of nonlinear differential systems. *IEEE Transactions on Automatic Control*, 22(6):909–921, 1977.

[20] Hochbruck M., Lubich C., Selhofer H. Exponential integrators for large systems of differential equations. *SIAM Journal of Scientific Computing*, 19(5):1552–1574, 1998.

[21] Balk I. Arnoldy based passive model order reduction algorithm. *Proceedings of the IEEE Conference on Electronic Packaging*, pages 251–254, 2000.

[22] Bauchau O. A., Craig J. I. Euler-Bernoulli Beam Theory. In Bauchau O. A., Craig J. I., editor, *Structural Analysis*, pages 173–221. Springer, Netherlands, 2009.

[23] Celledoni E., Moret I. A Krylov projection method for systems of ODEs. *Applied Numerical Mathematics*, 24(2-3):365–378, 1997.

[24] Berkooz G., Holmes P., Lumley J. The proper orthogonal decomposition in the analysis of turbulent flows. *Annual Review of Fluid Mechanics*, 25:539–575, 1993.

[25] Rewienski M. J. *A Trajectory Piecewise-Linear Approach to Model Order Reduction of Nonlinear Dynamical Systems*. PhD thesis, MIT, 2003.

[26] Willcox K., Peraire J. Balanced model reduction via the proper orthogonal decomposition. *AIAA*, 40(11):2323–2330, 2002.

[27] Yoo E. J. *Parametric Model Order Reduction for Structural Analysis and Control*. PhD thesis, Technical University of Munich, 2010.

[28] Benner P., Gugercin S., Willcox K. A survey of projection-based model reduction methods for parametric dynamical systems. *SIAM Reviews*, 57(4):483–531, 2015.

[29] Kumar D., Nagar S. K. Reducing power system models by Hankel norm approximation technique. *International Journal of Modelling and Simulation*, 33(3):139–143, 2013.

[30] Kumar D., Nagar S. K. Model reduction by extended minimal degree optimal Hankel norm approximation. *Applied Mathematical Modelling*, 38(11-12):2922–2933, 2014.

[31] Noor A. K. Recent advances in reduction methods for nonlinear problems. *Computers & Structures*, 13(1-3):31–44, 1981.

[32] Noor A. K. *Recent advances and applications of reduction methods*, 1994.

[33] Bathe K.-J., Wilson E. L. Solution methods for eigenvalue problems in structural mechanics. *International Journal for Numerical Methods in Engineering*, 6(2):213–226, 1973.

[34] Baur U., Benner P., Feng L. Model order reduction for linear and nonlinear systems: A system-theoretic perspective. *Archives of Computational Methods in Engineering*, 21(4):331–358, 2014.

[35] Davies J. M., Philip L. First-order generalised beam theory. *Journal of Constructional Steel Research*, 31:187–220, 1994.

[36] Feng L. Review of model order reduction methods for numerical simulation of nonlinear circuits. *Applied Mathematics and Computation*, 167:576–591, 2005.

[37] Meyer M. *Computational Model Order Reduction of Linear and Nonlinear Dynamical Systems: An Introduction*, 2006.

[38] Reddy J. N. *An Introduction to Nonlinear Finite Element Analysis*. Oxford University Press, Oxford, 2004.

[39] Kim N.-Ho. *Introduction to Nonlinear Finite Element Analysis*. Springer, New York, 2015.

[40] Chinesta F. Niroomandi S., Alfaro I., Gonzalez D., Cueto E. Model order reduction in hyperelasticity: A proper generalized decomposition approach. *International Journal for Numerical Methods in Engineering*, 96(3):129–149, 2013.

[41] Ladeveze P. *Nonlinear Computational Structural Mechanics*. Springer, New York, 1999.

[42] Nigro P. S. B., Anndif M., Teixeira Y., Pimenta P. M., Wriggers P. An adaptive model order reduction with Quasi-Newton method for nonlinear dynamical problems. *International Journal for Numerical Methods in Engineering*, 106(9):740–759, 2016.

[43] Brennan C., Condon M., Ivanov R. Model Order Reduction of Nonlinear Dynamical Systems. In Di Bucchianico A., Mattheij R., Peletier M., editor, *Progress in Industrial Mathematics at ECMI 2004*, pages 114–118. Springer, Berlin, Heidelberg, 2006.

[44] Feldmann P., Freund R. Efficient linear circuit analysis by Padé approximation via the Lanczos process. *IEEE Transactions on Computer-Aided Design*, 14:137–158, 1993.

[45] Kumari S., Taneja R. A review on order reduction of system using Routh approximation method. *International Journal of Research in Management, Science & Technology*, 3(2):631–644, 2015.

[46] Phillips J. R. Projection-based approaches for model reduction of weakly nonlinear time-varying systems. *IEEE Transactions on Computer-Aided Design*, 22(2):171–187, 2003.

[47] Rathinam M., Petzold L. R. A new look at proper orthogonal decomposition. *SIAM Journal of Numerical Analysis*, 41(5):1893–1925, 2003.

[48] Schardt R. *Verallgemeinerte Technische Biegetheorie*. Springer, Berlin, 1989.

[49] Dedden R.J. *Model Order Reduction using the Discrete Empirical Interpolation Method*. Master thesis, Delft University of Technology, 2012.

[50] Cirak F. Rüberg T. An immersed finite element method with integral equation correction. *International Journal for Numerical Methods in Engineering*, 86(1):93–114, 2011.

[51] Lall S., Marsden J.E., Glavaski S. Empirical model reduction of controlled nonlinear systems. *Proceeding of the 14th International Federation of Automatic Control World Congress*, 6:473–478, 1999.

[52] Lall S., Marsden J.E., Glavaski S. A subspace approach to balanced truncation for model reduction of nonlinear systems. *International Journal of Robust and Nonlinear Control*, 12(6):519–535, 2002.

[53] Volkwein S. Pod for nonlinear systems reduced-order modeling and error estimation. In *Model Reduction: Theory and Application*, Rocquencourt, France, 2007. CEA-EDF-INRIA School.

[54] Penzl T. Algorithms for model reduction of large dynamical systems. *Linear Algebra and its Application*, 415(2-3):322–343, 2006.

[55] Bui-Thanh T., Willcox K., Ghottas O., van Bloemen B. Goal-oriented, model-constrained optimization for reduction of large-scale systems. *Journal of Computational Physics*, 224(2):880–896, 2007.

[56] Schilders W., van der Vorst H. A., Rommes J. *Model Order Reduction: Theory, Research Aspects and Applications*. Springer, Berlin, Heidelberg, 2008.

[57] van Dooren P. Gramian Based Model Reduction of Large-Scale Dynamical Systems. In Griffiths D. F. Watson G. A., editor, *Numerical Analysis*, pages 231–247. Chapman & Hall/CRC, London, 2000.

[58] Gallivan K., Grimme E., van Dooren P. Padé approximation of large-scale dynamical systems with Lanczos methods. *Proceeding of the 33rd Conference on Decision and Control*, pages 443–448, 1994.

[59] Gallivan K., Grimme E., van Dooren P. Asymptotic waveform evaluation via a Lanczos method. *Applied Mathematics Letters*, 7(5):75–80, 1994.

[60] Freund R. W. Krylov-subspace methods for reduced-order modeling in circuit simulation. *Journal of Computational and Applied Mathematics*, 123(1–2):395–421, 2000.

[61] Freund R. W. Padé-type Model Reduction of Second-Order and Higher-Order Linear Dynamical Systems. In Benner P., Sorensen D. C., Mehrmann V., editor, *Dimension Reduction of Large-Scale Systems*, pages 191–223. Springer, Berlin, Heidelberg, 2005.

[62] Freund R. W. Recent Advances in Structure-Preserving Model Order Reduction. In Li P., Silveira L. M., Feldmann P., editor, *Simulation and Verification of Electronic and Biological Systems*, pages 43–70. Springer, Netherlands, 2011.

[63] Bai Z. Krylov subspace techniques for reduced-order modeling for large-scale dynamical systems. *Applied Numerical Mathematics*, 43(1-2):9–44, 2002.